American Mineralogist, Volume 63, pages 621–640, 1978

Mineral parageneses of eclogitic rocks and related mafic schists of the Piemonte ophiolite nappe, Breuil–St. Jacques area, Italian Western Alps[1]

W. G. ERNST

Department of Earth and Space Sciences
Institute of Geophysics and Planetary Physics
University of California, Los Angeles, California 90024

AND G. V. DAL PIAZ

Istituto di Geologia dell'Università
Via Giotto 1, 35100 Padova, Italy

Abstract

The principal unit exposed along the southern flank of the Matterhorn consists predominantly of Mesozoic calc-schists, greenstones, and serpentinized peridotites of the Piemonte ophiolite nappe. This complex is structurally underlain by the Pennine Monte Rosa nappe, and overlain by the Austroalpine Dent Blanche + Sesia–Lanzo nappe. Juxtaposed representatives of two petrotectonic units occur within the Piemonte ophiolitic complex: the structurally lower Zermatt–Saas unit, and the structurally higher Combin unit. The former represents metamorphosed oceanic crust + uppermost mantle of the Tethyan lithospheric plate, whereas the latter reflects a lithologic transition to the European continental margin. Although both tectonic entities have been subjected to pervasive greenschist-facies recrystallization, mainly of Eocene–early Oligocene age (the Lepontine event), the Zermatt–Saas unit in addition retains abundant relict Late Cretaceous (Early Alpine) eclogitic and blueschistic phase assemblages.

The chief minerals of the eclogites and related mafic schists, including 10 metabasalts and three metagabbros from the Zermatt–Saas unit as well as two greenschists and two metagabbros from the Combin unit, have been analyzed employing electron microprobe techniques. Chemical data are presented for 13 garnets, 11 omphacites, 12 sodic amphiboles, 24 calcic amphiboles, 19 epidotes, 12 white micas, 8 chlorites, 10 sodic plagioclases, and 6 sphenes. Textural relations presented previously indicate the prograde development of highest grade garnet + omphacite + rutile rocks, partly or completely converted to schists which display the successive newly-generated retrograde minerals glaucophane, epidote, barroisite, sphene, albite, chlorite + white micas, and actinolite. Only the culmination of the prograde relatively high-pressure metamorphism has been preserved, but a continuum of phase compatibilities marks the retrograde event. Employing experimentally-determined phase equilibrium and element fractionation data, and by analogy with oxygen isotope geothermometry of analogous parageneses, the following physical conditions have been estimated for the Breuil–St. Jacques area mineral assemblages: eclogites, 470 ± 50°C, 10 ± 2 kbar, a_{H_2O} very low; blueschists, 450 ± 50°C, >7 kbar, a_{H_2O} low; greenschists (prasinites), 400 ± 50°C, 3 ± 2 kbar, a_{H_2O} high. Barroisitic amphibolites appear to have formed over a range of *P–T* conditions intermediate between those quoted above for blueschists and greenschists and at moderate H_2O activities.

The presumed high-pressure Early Alpine prograde path is characteristic of subduction-zone metamorphism, whereas the better preserved retrograde *P–T* trajectory may represent nearly adiabatic decompression—evidently accompanying buoyant return of the subducted complex towards the surface after its detachment from the downgoing Tethyan lithospheric slab. The greenschist-facies overprinting, which according to isotopic age measurements is connected chiefly with the Lepontine metamorphic event, seems to be related to a post-collisional thermal reequilibration of the pile of nappes.

[1] Institute of Geophysics and Planetary Physics publication no. 1827.

0003–004X/78/0708–0621$02.00

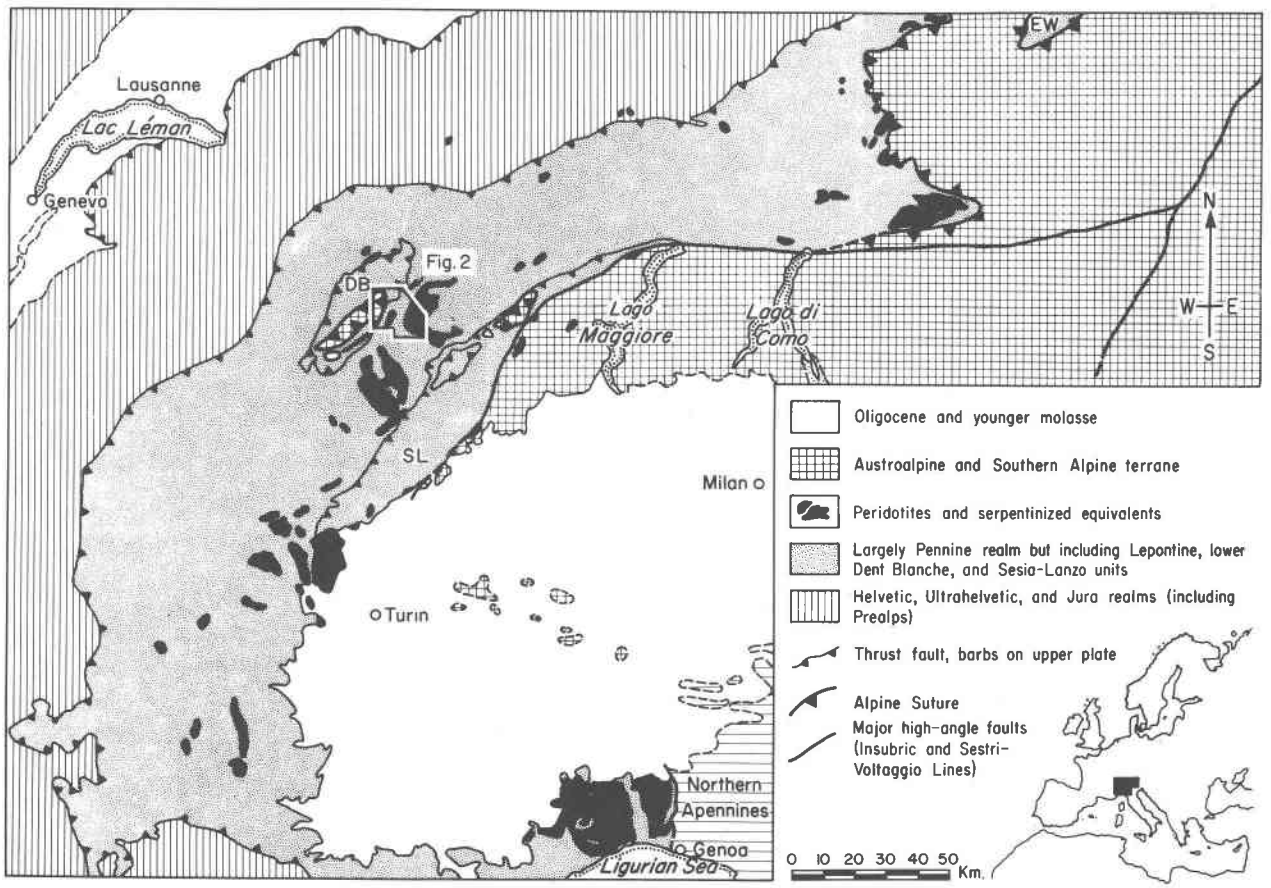

Fig. 1. Generalized map of the Western and Central Alps after Niggli *et al.* (1973). Thrust vergence is directed externally, away from the Po Plain. Late Mesozoic metamorphic and plate-tectonic units (Dal Piaz *et al.*, 1972; Dewey *et al.*, 1973), juxtaposed across the complex zone of the Alpine Suture (Ernst, 1971, 1973) are: southern plate = Austro-alpine + upper Dent Blanche + Southern Alpine terranes; northern (including Tethyan) plate = Helvetic + Lepontine + Pennine + lower Dent Blanche + Sesia–Lanzo terranes. Note that the latter two units were originally portions of the South Alpine plate, but apparently became detached and were subducted along with the more northerly terrane during the Late Cretaceous closure of Tethys (Ernst, 1973). As indicated by sparsely developed Early Alpine high-pressure mineral assemblages, this history may also apply to the presumably less deeply subducted upper Dent Blanche nappe (Dal Piaz *et al.*, 1972; Compagnoni *et al.*, 1975). Location of the Breuil–St. Jacques area is indicated as Fig. 2.

Introduction

As part of a U.S.–Italy Cooperative Project dealing with large-scale structures and relatively high-pressure metamorphism in the Italian Western Alps, we have investigated geologic and petrochemical features of the upper Valtournanche and Val d'Ayas, valleys situated directly south of the Matterhorn along the Swiss frontier. Geologic and general petrographic–petrologic relationships of this region—here designated the Breuil[2]–St. Jacques area—were detailed in an earlier portion of this study (Dal Piaz and Ernst, in press). The present report is mainly an electron microprobe study of the mineral assemblages of the mafic metamorphic rocks, and attempts to elucidate the P–T history of recrystallization for this portion of the Pennine terrane. Brief plate-tectonic interpretations of the data are also put forward.

The regional geologic setting of the investigated area is shown in Figure 1. Studied rocks belong to the calc–schist + greenstone complex of the Pennine Piemonte ophiolite nappe (Franchi, 1898), the chief petrotectonic unit in the district. This complex is sandwiched between the structurally overlying Austroalpine Dent Blanche + Sesia–Lanzo nappes and the underlying Pennine Monte Rosa + Gran Paradiso + Gran San Bernardo nappes. The Piemonte ophiolite nappe itself consists of two major tectonic units, separated by a sheared zone of blastomylonites and tectonic slices. The structurally

[2] The ancient village of Breuil is now known as Cervinia.

lower *Zermatt–Saas* unit consists chiefly of mid and late(?) Mesozoic metaophiolites of oceanic affinities, radiolarites, and calc–schists. The structurally higher *Combin* unit represents an early Mesozoic continental-margin series of metasedimentary strata overlain by mid and late(?) Mesozoic interbedded calc–schists and metabasaltic horizons. Generalized geologic relationships and sample localities are presented in Figure 2. The reader is referred to the paper by Dal Piaz and Ernst (in press) for descriptions of the various lithologic assemblages, structural relationships, and more complete citations of earlier works.

Mineral parageneses

Mafic metamorphic rocks of both Zermatt–Saas and Combin units are chemically indistinguishable (Dal Piaz *et al.*, 1972 and in press; Kienast, 1973). They range in bulk composition from oceanic tho-

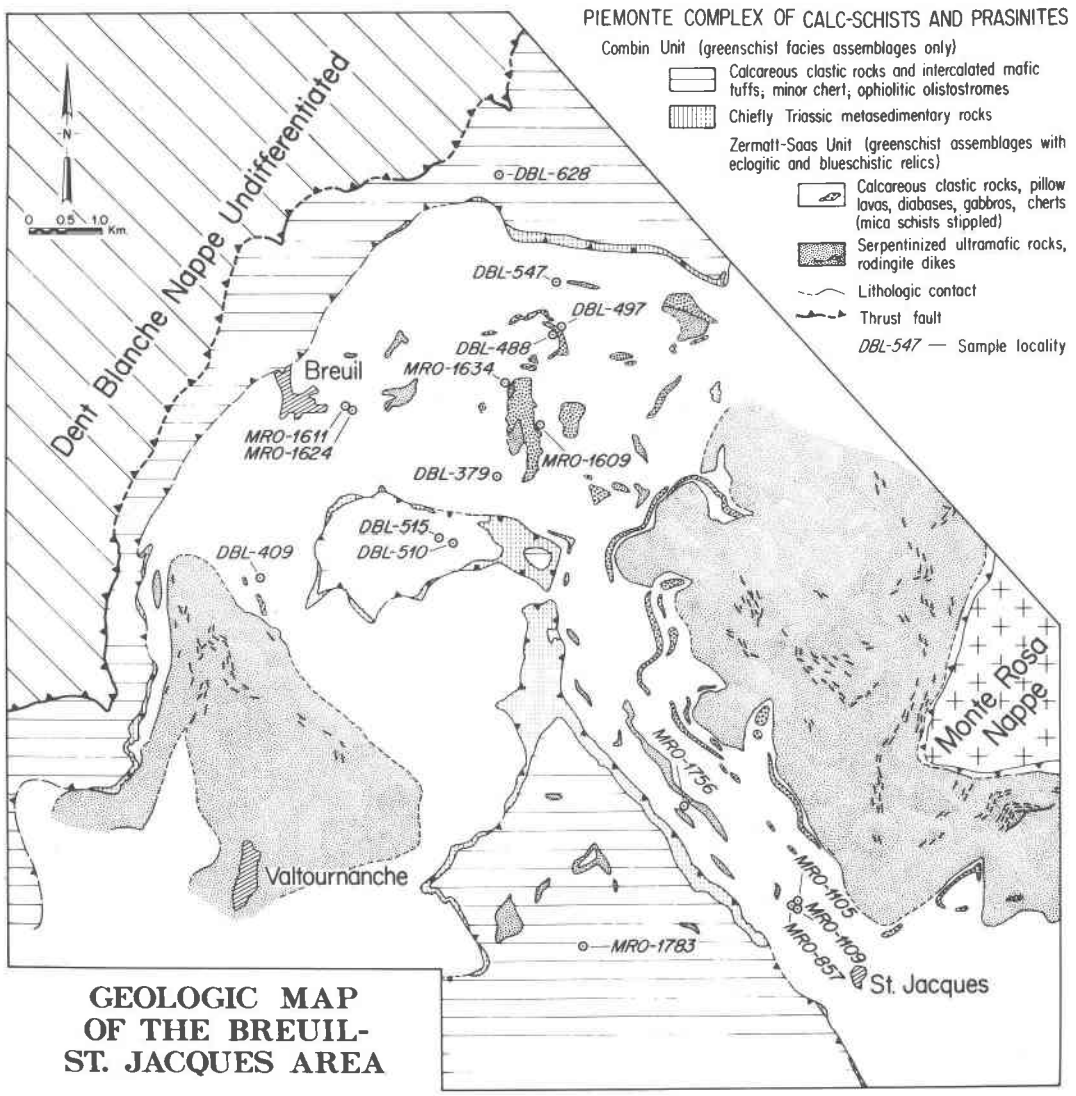

Fig. 2. Tectonic and lithologic map of the Breuil–St. Jacques area, showing sample locations (Dal Piaz and Ernst, in press). The Combin unit of the Piemonte nappe consists mainly of calc–schists and interbedded greenschists (metabasaltic flows and/or tuffs and tuffites) with minor chert and tectonic lenses and/or olistostrome deposits of metagabbro + serpentinite. This sequence covers the pre-ophiolitic basal complex of continental affinity, chiefly Triassic and Liassic carbonates, but locally including Permian(?) strata. The Zermatt–Saas unit is composed of pervasively serpentinized basal ultramafites, discontinuous metagabbros and widely distributed metabasaltic rocks, containing interbedded conglomeratic mica schists and tectonic mélanges of the Garten–Rifelberg formation (coarsely stippled), plus a sedimentary cover of ankeritic mica schists with rare marbles and metacherts. The Zermatt–Saas unit of the Piemonte nappe exhibits an Early Alpine eclogitic stage of metamorphism, succeeded by glaucophanic, barroisitic, and actinolitic stages of retrogression, whereas the Combin unit shows a greenschist-facies metamorphic overprinting with very scarce Na–amphibole relics.

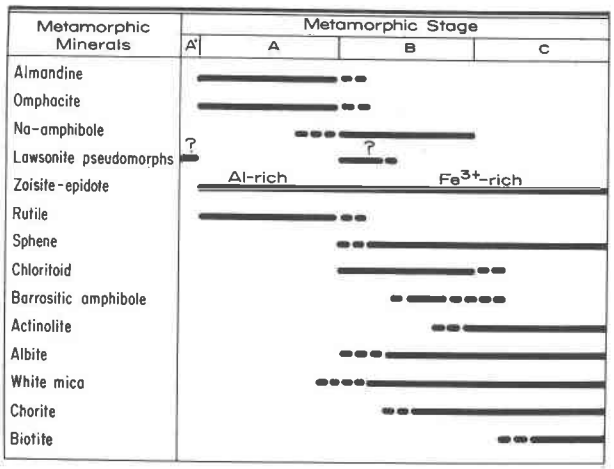

Fig. 3. Schematic paragenetic diagram illustrating mineral assemblages and metamorphic stages in the Zermatt–Saas and Combin metabasites from the Breuil–St. Jacques area. Dashed lines signify rare or questionable occurrences. The persistence of metastable relics is not shown. Stages A, B, and C are all preserved in rocks of the Zermatt–Saas unit, whereas the Combin prasinites, which contain rare relict sodic amphiboles as well as minor hornblendic amphiboles, reflect dominantly stage-C recrystallization. It is not clear whether the hypothesized production of lawsonite (now represented by zoisite–epidote + white mica prismatic intergrowths) occurred prior to stage A, or during stage B, or both.

leiites to slightly alkaline basalts (Dal Piaz and Ernst, in press). The Zermatt–Saas and Combin metabasaltic mineral assemblages, however, exhibit remarkable contrasts (Bearth, 1953, 1976; Dal Piaz and Ernst, in press). Observed parageneses deduced from these petrographic studies are illustrated schematically in Figure 3.

The Zermatt–Saas rocks contain relics of an Early Alpine eclogitic phase assemblage (= stage A), succeeded in turn by the production of blueschists (= stage B), barroisitic albite-bearing amphibolites and finally prasinites—*i.e.*, porphyroblastic albite-bearing greenschists—(= stage C) of Lepontine metamorphic age. In contrast, although the Combin unit displays a few relics of Na–amphiboles, textural relations demonstrate that, for the most part, pre-existing igneous assemblages were converted directly to prasinitic associations. Radiometric data indicate that the Early Alpine recrystallization took place about 90–80 m.y. ago, whereas the Lepontine thermal event culminated about 38 m.y. ago (Hunziker and Bearth, 1969; Hunziker, 1974; Bocquet *et al.*, 1974; Delaloye and Desmons, 1976).

The Zermatt–Saas unit contains blocky aggregates of zoisite–epidote + white mica resembling pre-existing lawsonite porphyroblasts. Presuming that these intergrowths reflect pseudomorphism of prismatic lawsonite, it is unclear whether this hydrous Ca–Al silicate preceded the stage A eclogitic period of crystallization (*i.e.*, hypothetical prograde stage A′; see Fry and Fyfe, 1971), or formed during the retrograde conversion of these rocks to glaucophane schists during stage B (Bearth, 1973), or both. The back-reaction evidently took place under continuously changing conditions, as indicated by the gradual conversion of glaucophanic mafic schists to barroisitic hornblende- then actinolitic amphibole-bearing schists during stage C (Wetzel, 1974; Dal Piaz and Ernst, in press).

Compositions of coexisting phases

Compositions of minerals from 17 eclogites and related metabasaltic rocks of the Breuil–St. Jacques area were obtained by electron microprobe analysis. Analytical techniques were described previously (Ernst, 1976). Bulk-rock major-element chemistries and mineral assemblages of the investigated samples are presented by Dal Piaz and Ernst (in press). The Zermatt–Saas rocks studied are eclogites and glaucophane eclogites (MRO-857, MRO-1105, MRO-1609, MRO-1611, DBL-379, DBL-497), hyaloclastitic glaucophanites (MRO-1634, DBL-409), thoroughly retrograded eclogites (MRO-1624, DBL-488), and metagabbros (MRO-1109, MRO-1756, DBL-547). Specimens chosen for electron microprobe analysis from the tectonically overlying Combin unit include two metagabbros (DBL-515, DBL-628) and two prasinitic metavolcanics (MRO-1783, DBL-510). Sample locations are indicated in Figure 2.

Iron contents were somewhat arbitrarily calculated as entirely ferric for epidote and plagioclase, half ferric for Na–clinopyroxene and glaucophane, and all ferrous for the other analyzed phases. This method tends to overestimate the Fe^{3+} contents of sodic amphiboles and the Fe^{2+} contents of calcic amphiboles. Unfortunately, because of the presence of the A structural site in amphiboles (which may be empty, fully or only partly occupied by monovalent cations), and the possibility of variable dehydrogenation of the O3 anion (normally hydroxyl), a severe problem exists in calculating the amphibole ferric/ferrous ratio, and it cannot be performed unambiguously. However, the microprobe data seem to be quite comparable, both in terms of accuracy and precision, to wet-chemical and Mössbauer analyses of similar rock-forming silicates in the literature (see discussion by Ernst, 1976).

The computer output was provided in terms of

Table 1. Electron microprobe analyses of garnets from eclogitic parageneses, Breuil–St. Jacques area

	Sample Number												
Oxide	MRO-857	MRO-1105	MRO-1109	MRO-1609	MRO-1611	MRO-1624	MRO-1634	MRO-1756	DBL-379	DBL-409	DBL-488	DBL-497c	DBL-497r
SiO_2	37.34	37.38	36.47	36.93	37.56	36.98	37.02	36.65	36.99	36.85	37.48	37.35	37.35
Al_2O_3	23.50	23.78	23.42	23.87	24.19	23.72	23.48	23.42	23.53	23.91	23.87	23.78	23.73
TiO_2	0.10	0.12	0.06	0.06	0.04	0.04	0.12	0.10	0.07	0.10	0.12	0.11	0.05
Cr_2O_3	0.00	0.01	0.00	0.00	0.00	0.00	0.09	0.00	0.00	0.07	0.13	0.00	0.00
FeO	30.71	31.18	29.93	28.38	29.32	31.56	29.77	30.82	30.12	31.78	30.04	27.98	29.76
MgO	1.95	2.14	1.84	3.00	2.61	1.87	2.43	1.61	2.04	1.66	1.82	1.57	2.25
MnO	0.57	0.32	1.78	1.59	1.18	0.87	1.44	1.47	1.88	1.17	1.09	2.39	1.27
CaO	8.30	8.03	7.87	7.29	8.05	7.34	7.71	7.86	7.92	6.91	8.42	9.84	7.89
Na_2O	0.01	0.01	0.00	0.02	0.02	0.01	0.03	0.00	0.00	0.00	0.02	0.02	0.02
K_2O	0.00	0.00	0.00	0.00	0.00	0.00	0.01	0.00	0.00	0.01	0.01	0.00	0.00
Total	102.47	102.96	101.37	101.14	102.97	102.38	102.08	101.91	102.54	102.44	102.98	103.03	102.31
Si	2.903	2.891	2.877	2.887	2.889	2.887	2.888	2.881	2.883	2.878	2.896	2.888	2.901
Al^{IV}	0.097	0.109	0.123	0.113	0.111	0.113	0.112	0.119	0.117	0.122	0.104	0.112	0.099
Al^{VI}	2.057	2.059	2.054	2.075	2.083	2.069	2.046	2.050	2.044	2.079	2.070	2.054	2.073
Ti	0.006	0.007	0.004	0.004	0.002	0.002	0.007	0.006	0.004	0.006	0.007	0.006	0.003
Cr	0.000	0.001	0.000	0.000	0.000	0.000	0.005	0.000	0.000	0.004	0.008	0.000	0.000
Fe^{2+}	1.997	2.017	1.975	1.855	1.886	2.060	1.942	2.026	1.963	2.078	1.941	1.809	1.933
Mg	0.226	0.247	0.216	0.350	0.299	0.217	0.283	0.189	0.236	0.193	0.210	0.181	0.261
Mn	0.038	0.021	0.118	0.106	0.077	0.058	0.095	0.098	0.124	0.077	0.072	0.157	0.084
Ca	0.692	0.666	0.666	0.610	0.663	0.614	0.644	0.662	0.662	0.579	0.697	0.815	0.656
Na	0.001	0.001	0.000	0.003	0.003	0.001	0.004	0.000	0.000	0.000	0.003	0.003	0.003
K	0.000	0.000	0.000	0.000	0.000	0.000	0.001	0.000	0.000	0.001	0.001	0.000	0.000

c = core; r = rim

oxide weight percents, and corresponding cation proportions based on one formula unit; all data were corrected for drift, background, atomic number, fluorescence, and absorption. Analyses are presented in Tables 1–9. The discussion which follows focusses on cation amounts per formula unit. An attempt was made to investigate homogeneous phases, but in samples where significant chemical zoning was detected cores and/or rims were analyzed, and are so designated in the tables.

Garnet

Analyses of eleven homogeneous garnets and one core + rim pair (sample DBL-497) from the Zermatt–Saas unit are presented in Table 1. Although the oxide totals are unusually high, ranging between 101.14–103.03 weight percents, cation sums based on 12 oxygens range only between the extreme values 8.003–8.033, very close to the stoichiometric value of 8.00. Minor amounts of aluminum are assigned to tetrahedral sites, averaging 0.112 based on one formula unit; Al^{VI} averages 2.062, slightly in excess of the ideal value of 2.00. Perhaps the high oxide weight percent totals reflect an overestimation of the aluminum actually present in these garnets; this would account for the high Al^{IV} and Al^{VI} values. Alkalis, Cr, and Ti are present in insignificant proportions, as seen from Table 1.

With aluminum apparently occupying all of the six-coordinated cation positions, ferric iron contents must be very low, hence compositional variations of these garnets may be shown adequately in terms of the Ca, Fe^{2+}, Mg, and Mn proportions. As shown by Figure 4, analyzed values cluster tightly around the average composition $Alm_{66.5}Py_{8.1}Gross_{22.5}Spess_{2.9}$. These garnets have slightly higher Alm and lower Py contents than those analyzed by Bearth (1967, 1973) in the Zermatt area just to the north. The chemical zonation measured in sample DBL-497 is from a calcium + manganese-rich core to an iron + magnesium-rich rim, analogous to other relatively low-temperature eclogitic parageneses (Råheim and Green, 1975; Ernst, 1976). There is also an indication from the one analyzed core-rim pair that the Mg/Fe^{2+} ratio increased during the course of crystallization (Fig. 4a), although the absolute changes in cation proportions of Ca, Fe^{2+}, Mg, and Mn are rather small.

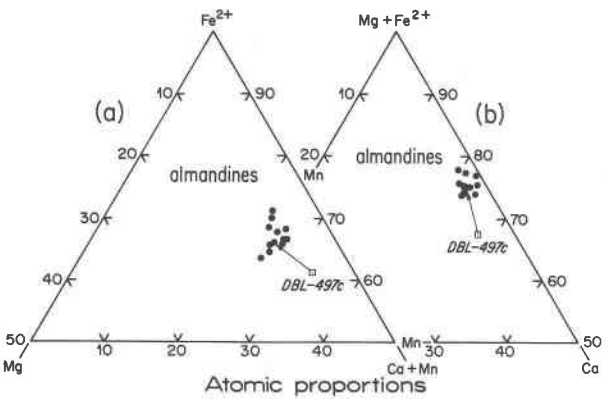

Fig. 4. Proportions of cations occupying the large eight-coordinated sites in Breuil-St. Jacques garnets from eclogites and related rocks from the Zermatt-Saas unit in terms of: (a) Fe^{2+}–Mg–(Ca + Mn), and (b) (Mg + Fe^{2+})–Mn–Ca. The garnet core of specimen DBL-497 is indicated by the square; an arrow points to the analyzed rim composition. Rim and homogeneous compositions are shown by black dots. Note that only the Fe^{2+}-rich portions of the diagrams are illustrated.

Omphacite[3]

Sodic pyroxene analyses from nine Zermatt–Saas rocks are listed in Table 2. For samples MRO-857 and MRO-1105, grains in different portions of the microprobe slide were investigated (multiple grain analyses for a single rock are indicated by prime symbols in the tabulations). Based on six oxygens, cation totals range from 3.953 to 4.012 and average 3.981, in very good agreement with the stoichiometric value of 4.00. Total aluminum contents of these eleven clinopyroxenes range from 0.353–0.575; Al is virtually all octahedrally-coordinated, Al^{IV} averaging only 0.009 based on one formula unit. Potassium is absent, traces of Cr occur in only a few specimens, and Ti and Mn averages only 0.001 and 0.002, respectively, per six oxygens.

[3] As employed in this paper, "omphacite" refers to a clinopyroxene chemically intermediate among the four end members Jd, Ac, Di, and Hd.

Table 2. Electron microprobe analyses of Na-clinopyroxenes from eclogitic parageneses, Breuil-St. Jacques area

	Sample Number										
Oxide	MRO-857	MRO-857'	MRO-1105	MRO-1105'	MRO-1109	MRO-1609	MRO-1611	DBL-379	DBL-409	DBL-497	DBL-547
SiO_2	54.15	54.23	54.96	55.35	55.03	55.69	54.92	54.54	54.64	55.41	56.02
Al_2O_3	8.14	9.26	8.41	9.06	10.72	13.70	12.08	8.81	9.82	9.81	12.25
TiO_2	0.05	0.06	0.04	0.07	0.06	0.05	0.05	0.04	0.06	0.04	0.05
Cr_2O_3	0.04	0.00	0.00	0.00	0.00	0.00	0.00	0.04	0.00	0.00	0.12
Fe_2O_3	5.26	4.64	4.65	4.93	3.84	3.90	4.56	5.16	6.74	4.91	1.83
FeO	4.73	4.17	4.18	4.44	3.46	3.51	4.10	4.64	6.07	4.42	1.65
MgO	7.20	7.14	7.39	6.64	6.68	4.45	5.12	6.34	4.26	5.97	8.91
MnO	0.00	0.00	0.05	0.10	0.03	0.05	0.02	0.04	0.06	0.09	0.11
CaO	12.14	11.66	12.83	12.24	11.98	8.96	9.72	12.42	8.86	11.98	12.92
Na_2O	7.08	7.36	6.52	6.56	7.11	8.39	8.24	6.76	8.51	6.83	6.92
K_2O	0.00	0.00	0.00	0.00	0.00	0.00	0.00	0.00	0.00	0.00	0.00
Total	98.79	98.52	99.03	99.39	98.91	98.70	98.81	98.75	99.02	99.46	100.78
Si	1.990	1.986	2.002	2.006	1.989	1.996	1.987	1.998	2.005	2.004	1.954
Al^{IV}	0.010	0.014	0.000	0.000	0.011	0.004	0.013	0.002	0.000	0.000	0.046
Al^{VI}	0.342	0.385	0.361	0.387	0.445	0.575	0.502	0.378	0.424	0.418	0.458
Ti	0.001	0.002	0.001	0.002	0.002	0.001	0.001	0.001	0.002	0.001	0.001
Cr	0.001	0.000	0.000	0.000	0.000	0.000	0.000	0.001	0.000	0.000	0.003
Fe^{3+}	0.146	0.128	0.127	0.135	0.105	0.105	0.124	0.142	0.187	0.134	0.048
Fe^{2+}	0.146	0.128	0.127	0.135	0.105	0.105	0.124	0.142	0.187	0.134	0.048
Mg	0.394	0.390	0.401	0.358	0.360	0.238	0.276	0.346	0.233	0.322	0.464
Mn	0.000	0.000	0.002	0.003	0.001	0.002	0.001	0.001	0.002	0.003	0.004
Ca	0.478	0.457	0.501	0.475	0.464	0.344	0.377	0.488	0.348	0.465	0.483
Na	0.504	0.522	0.460	0.460	0.498	0.583	0.577	0.480	0.604	0.479	0.469
K	0.000	0.000	0.000	0.000	0.000	0.000	0.000	0.000	0.000	0.000	0.000

The sum of Ca + Na ranges from 0.927 to 0.982, averaging 0.956; this indicates that there is very minor solid solution (averaging about 4.4 percent) towards En + Fs end-members in Valtournanche and Val d'Ayas clinopyroxenes. Figure 5a shows that the Na/Ca ratios of these clinopyroxenes are close to, but in most cases slightly exceed, 1/1. Figure 5b demonstrates that the corresponding $(Al^{VI} + Fe^{3+})/(Mg + Fe^{2+})$ ratios also are close to but a trifle larger than unity. Coupled with cation totals which are insignificantly less than the ideal formula value, this probably means that the ferric-iron contents of the omphacites have been only very slightly overestimated, if at all. As is clear from Table 2 and Figure 5, the omphacites are of relatively constant chemistry. Ignoring the small amounts of (En + Fs) solid solution, the average composition of these omphacites is $Jd_{42}Ac_{12}Di_{34}Hd_{12}$—nearly identical to the average ($Jd_{40.5}Ac_{13.5}Di_{34}Hd_{12}$) of five Zermatt sodic pyroxenes reported by Bearth (1973). To some extent this close similarity supports the assumption of equal proportions of ferrous and ferric iron in Valtournanche and Val d'Ayas omphacites.

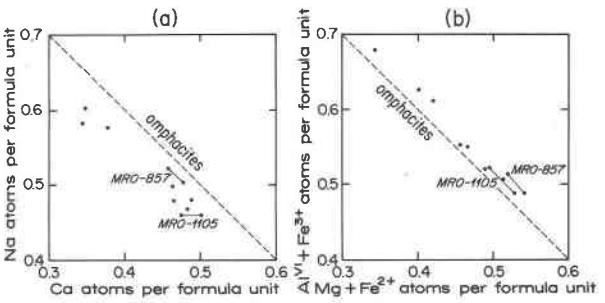

Fig. 5. Proportions of six-coordinated cations per six oxygens in Breuil–St. Jacques clinopyroxenes from eclogites and related rocks from the Zermatt–Saas unit: (a) occupancy of the large M2 site; (b) occupancy of the smaller M1 structural position. Dashed lines indicate the locus of 100 percent filling of the site by the plotted cations; slight but systematic deviations from the lines reflect small proportions of $(Mg + Fe^{2+})$ residing in M2. Solid lines connect analyses of different grains in samples MRO-857 and MRO-1105. Note that only intermediate (Jd + Ac)–(Di + Hd) compositional ranges are graphed.

Glaucophane

Twelve analyses of sodic amphibole from seven different rocks of the Zermatt–Saas unit are presented in Table 3. Of this group, four represent core

Table 3. Electron microprobe analyses of Na-clinoamphiboles from eclogitic parageneses, Breuil–St. Jacques area

	Sample Number											
Oxide	MRO-857c	MRO-857r	MRO-857'c	MRO-1609	MRO-1611c	MRO-1611r	MRO-1634	DBL-379c	DBL-379r	DBL-409	DBL-497c	DBL-497r
SiO_2	57.10	57.64	57.18	57.15	57.20	57.50	56.79	56.28	55.75	53.50	57.36	57.16
Al_2O_3	11.67	11.90	11.40	12.76	12.37	13.06	10.62	9.82	11.77	11.85	11.08	12.85
TiO_2	0.02	0.02	0.00	0.00	0.02	0.02	0.02	0.02	0.02	0.09	0.03	0.06
Cr_2O_3	0.00	0.03	0.00	0.00	0.00	0.00	0.00	0.00	0.03	0.00	0.00	0.00
Fe_2O_3	4.47	4.69	4.54	5.06	4.44	4.84	5.87	6.08	6.49	8.45	5.76	5.36
FeO	4.02	4.22	4.08	4.55	3.99	4.36	5.28	5.47	5.84	7.59	5.19	4.82
MgO	12.17	11.77	12.02	8.91	10.49	9.23	9.55	9.92	8.49	7.18	9.56	9.01
MnO	0.00	0.02	0.01	0.02	0.00	0.02	0.09	0.08	0.09	0.05	0.05	0.09
CaO	1.29	1.17	1.47	0.56	0.58	0.76	0.90	1.77	1.25	1.74	0.69	1.14
Na_2O	6.65	6.68	6.57	6.67	6.80	6.73	6.11	6.13	6.52	6.08	6.57	6.41
K_2O	0.00	0.01	0.01	0.00	0.02	0.01	0.03	0.03	0.03	0.07	0.01	0.00
H_2O	2.00	2.00	2.00	2.00	2.00	2.00	2.00	2.00	2.00	2.00	2.00	2.00
Total	99.39	100.15	99.27	97.68	97.91	98.53	97.26	97.60	98.28	98.60	98.30	98.90
Si	7.793	7.810	7.818	7.912	7.884	7.887	7.959	7.913	7.797	7.594	7.948	7.849
Al^{IV}	0.207	0.190	0.182	0.088	0.116	0.113	0.041	0.087	0.203	0.406	0.052	0.151
Al^{VI}	1.670	1.710	1.654	1.993	1.893	1.998	1.713	1.539	1.737	1.576	1.758	1.928
Ti	0.001	0.001	0.000	0.000	0.002	0.002	0.002	0.002	0.002	0.010	0.003	0.006
Cr	0.000	0.002	0.000	0.000	0.000	0.000	0.000	0.000	0.004	0.000	0.000	0.000
Fe^{3+}	0.459	0.478	0.467	0.527	0.460	0.500	0.619	0.643	0.683	0.902	0.601	0.554
Fe^{2+}	0.459	0.478	0.467	0.527	0.460	0.500	0.619	0.643	0.683	0.902	0.601	0.554
Mg	2.475	2.376	2.449	1.837	2.153	1.886	1.993	2.077	1.768	1.518	1.973	1.844
Mn	0.000	0.001	0.001	0.002	0.000	0.002	0.011	0.010	0.011	0.006	0.006	0.011
Ca	0.188	0.169	0.215	0.083	0.086	0.112	0.136	0.267	0.188	0.265	0.103	0.168
Na	1.757	1.754	1.740	1.788	1.816	1.788	1.659	1.670	1.764	1.669	1.762	1.704
K	0.000	0.001	0.001	0.000	0.004	0.002	0.005	0.005	0.005	0.013	0.002	0.000

c = core; r = rim

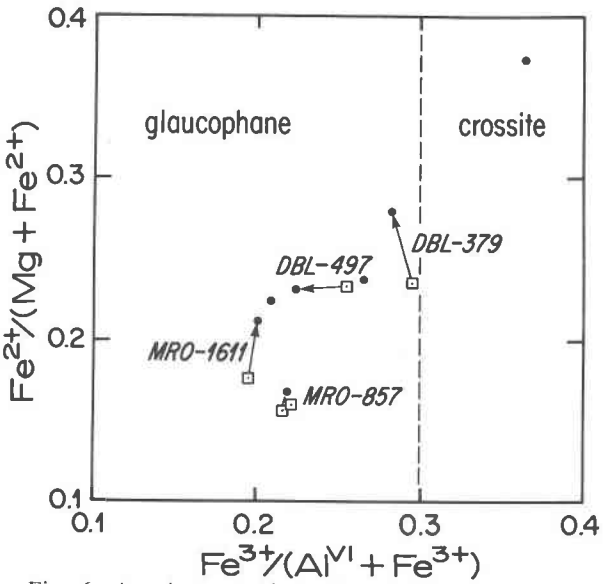

Fig. 6. Atomic proportions of six-coordinated cations in Breuil-St. Jacques Na-amphiboles from eclogites and related rocks from the Zermatt-Saas unit. Occupants of chiefly M2 structural sites are plotted along the ordinate, principally occupants of M1 + M3 along the abscissa. Rim and homogeneous compositions are shown by black dots. Glaucophane cores are indicated by squares; arrows point to analyzed rim compositions. For sample MRO-857, cores were analyzed in two different parts of the microprobe section. The dashed line denotes the classificational boundary between glaucophane *sensu stricto* and crossite (Miyashiro, 1957). Note that only a small portion of the sodic amphibole quadrilateral is presented.

+ rim pairs (samples MRO-857, MRO-1611, DBL-379, and DBL-497) and, in addition, cores of glaucophane from another part of section MRO-857 were probed. Recorded oxide totals are rather low, averaging 98.49 weight percent. However, cation proportions based on one formula unit appear to be reasonable: the range of total cations is 14.757–15.009 and averages 14.858, close to the ideal value of 15.00 (in general, glaucophanes tend to possess a vacant A structural site). Slightly low cation totals probably reflect an overestimation of the Fe^{3+}/Fe^{2+} ratio in these sodic amphiboles.[4] The assumption of high ferric-iron proportions also tends to increase the aluminum assigned to tetrahedral coordination, but Al^{IV} averages only 0.153 per 24 anions whereas Al^{VI} predominates, averaging 1.764.

Based on one formula unit, the average contents of Ti (= 0.003), Cr (= 0.001), Mn (= 0.005), and K (= 0.003) are negligible in the sodic amphiboles of the Breuil–St. Jacques area. Calcium and sodium

[4] Except for sample DBL-379, single crystal X-ray diffraction studies have been performed on all analyzed sodic amphiboles by Ungaretti *et al.* (1977). Their results suggest that our Fe^{3+}/Fe^{2+} ratios (Table 3) are somewhat high. The overestimation seems to be especially large in sample DBL-409 which plots along with the other amphiboles in the glaucophane field. The negligible calcium content of these Na-amphiboles has been confirmed by the X-ray work of Ungaretti *et al.*

Table 4. Electron microprobe analyses of Ca-clinoamphiboles from eclogitic parageneses, Breuil-St. Jacques area

	Sample Number											
Oxide	MRO-857	MRO-1105	MRO-1105'	MRO-1105"	MRO-1105"'	MRO-1109	MRO-1109'	MRO-1109"	MRO-1109"'	MRO-1609	MRO-1611	MRO-1624
SiO_2	53.88	43.43	50.26	49.89	53.67	43.90	48.36	51.68	54.94	49.38	51.23	46.21
Al_2O_3	4.19	12.77	9.79	8.81	5.51	13.27	9.29	7.20	5.27	7.35	4.16	10.15
TiO_2	0.06	0.18	0.18	0.19	0.13	0.14	0.09	0.12	0.08	0.15	0.07	0.34
Cr_2O_3	0.00	0.00	0.00	0.00	0.00	0.00	0.00	0.00	0.00	0.00	0.00	0.00
FeO	9.80	19.89	13.98	15.29	11.59	18.18	15.16	11.49	7.51	12.45	12.93	17.18
MgO	15.93	6.85	9.95	9.78	12.38	7.25	10.05	13.09	15.87	11.73	12.79	9.10
MnO	0.13	0.22	0.14	0.11	0.12	0.25	0.24	0.22	0.16	0.10	0.12	0.19
CaO	9.17	9.48	7.77	8.57	9.55	7.93	8.34	9.42	9.58	8.89	10.03	8.00
Na_2O	2.33	3.01	3.39	2.83	2.13	3.44	2.50	2.28	1.74	3.33	2.07	3.07
K_2O	0.05	0.08	0.15	0.19	0.06	0.34	0.13	0.18	0.07	0.20	0.06	0.36
H_2O	2.00	2.00	2.00	2.00	2.00	2.00	2.00	2.00	2.00	2.00	2.00	2.00
Total	97.54	97.91	97.61	97.65	97.14	96.70	96.15	97.67	97.20	95.58	95.47	96.60
Si	7.786	6.659	7.395	7.400	7.829	6.737	7.288	7.533	7.847	7.430	7.715	7.045
Al^{IV}	0.214	1.341	0.605	0.600	0.171	1.263	0.712	0.467	0.153	0.570	0.285	0.955
Al^{VI}	0.500	0.966	1.093	0.939	0.776	1.137	0.937	0.769	0.734	0.733	0.454	0.869
Ti	0.007	0.020	0.020	0.021	0.014	0.016	0.010	0.013	0.009	0.017	0.008	0.038
Cr	0.000	0.000	0.000	0.000	0.000	0.000	0.000	0.000	0.000	0.000	0.000	0.000
Fe^{2+}	1.184	2.550	1.720	1.897	1.414	2.333	1.911	1.401	0.897	1.567	1.628	2.190
Mg	3.430	1.566	2.182	2.162	2.691	1.659	2.259	2.845	3.378	2.631	2.871	2.069
Mn	0.016	0.029	0.018	0.014	0.015	0.032	0.030	0.027	0.019	0.013	0.016	0.025
Ca	1.420	1.557	1.224	1.361	1.493	1.304	1.346	1.471	1.466	1.433	1.618	1.307
Na	0.653	0.896	0.967	0.814	0.603	1.023	0.731	0.643	0.481	0.971	0.605	0.906
K	0.009	0.015	0.028	0.035	0.011	0.067	0.025	0.033	0.013	0.038	0.011	0.070

contents range from 0.083–0.267 and 1.659–1.816, respectively, indicating an average of about nine percent Ca occupancy of M4, the remaining 91 percent being Na. Ignoring this small degree of solid solution towards calcic amphiboles, chemical variations of the sodic amphiboles are plotted in Figure 6. Clearly these amphiboles approach the $Na_2Mg_3Al_2Si_8O_{22}(OH)_2$ end-member in composition. Chemical zoning evidently is not pronounced, but tends to enrich the grain margins in $Na_2Fe^{2+}_3Al_2Si_8O_{22}(OH)_2$ relative to the cores.

Actinolite–hornblende

Analyses of 24 Ca-amphiboles from 17 different rocks are presented in Table 4. In three specimens, MRO-1105, MRO-1109, and DBL-628, a distinct paragenetic sequence of amphibole compositions was measured. Samples DBL-510, DBL-515, and DBL-628 are from the Combin unit; all other analyzed Ca-amphiboles are from the Zermatt–Saas unit. The table shows that oxide totals for all of the analyzed Ca-amphiboles are very low, averaging only 97.38 weight percent. In part this phenomenon may reflect the fact that a substantial proportion of the iron is actually Fe^{3+}, rather than exclusively divalent as assumed. Nevertheless, the total number of cations per formula unit ranges from 14.935 to 15.599, essentially within the ideal stoichiometric 15.00–16.00 range appropriate for actinolite–hornblende solid solutions. Cations present in these amphiboles in small but variable amounts, and their average concentrations based on 24 anions, are as follows: Ti = 0.015, Cr = 0.001, Mn = 0.024, and K = 0.030. These constituents are less abundant in the high-Si, low-Al actinolites compared to the more hornblendic amphiboles.

Complex chemical variations in the analyzed calcic amphiboles occur among the other cations. Iron–magnesium variation is quite large; the $Fe^{2+}/(Mg + Fe^{2+})$ ratio ranges from 0.105 to 0.620, probably chiefly as a function of rock bulk composition. The sum of cations assigned to octahedral sites is relatively constant, however, averaging 5.084—close to the ideal value of 5.00.

Ignoring minor potassium, the Ca and Na occupancies of the M4 and A structural positions are illustrated in Figure 7a. Analyzed Ca-amphiboles appear to be intermediate members of the barroisite–actinolite series. Where compositional variation occurs, later members of the series are much more actinolitic than the earlier hornblendes. This relationship is also shown in Figure 7b as a plot of Al^{IV} *vs.* Al^{VI}; the aluminum is approximately equally divided between four-fold and six-fold structural sites, as is

Table 4. (continued)

Oxide	MRO-1634	MRO-1756	DBL-379	DBL-409	DBL-488	DBL-497	DBL-510*	DBL-515*	DBL-547	DBL-628*	DBL-628'*	DBL-628''*
	Sample Number											
SiO_2	46.01	50.92	46.95	45.59	49.45	49.17	54.12	53.41	56.51	48.03	55.34	55.52
Al_2O_3	11.67	7.91	9.94	12.78	9.97	10.62	2.76	5.94	2.90	9.21	1.61	0.54
TiO_2	0.35	0.11	0.22	0.29	0.11	0.20	0.03	0.08	0.02	0.09	0.00	0.00
Cr_2O_3	0.00	0.00	0.03	0.04	0.05	0.00	0.05	0.09	0.00	0.00	0.00	0.00
FeO	16.70	11.69	15.34	17.62	12.36	13.69	13.08	5.35	4.41	12.47	8.73	9.40
MgO	8.32	12.07	9.69	7.58	11.29	10.03	13.15	19.42	21.05	13.42	18.33	18.33
MnO	0.29	0.20	0.19	0.09	0.21	0.22	0.30	0.26	0.13	0.24	0.25	0.20
CaO	6.85	8.96	7.84	6.93	9.22	7.73	11.85	11.19	11.77	9.23	12.11	12.67
Na_2O	4.25	2.31	3.71	4.27	2.13	3.52	0.51	1.71	1.03	2.95	0.52	0.18
K_2O	0.29	0.14	0.15	0.38	0.16	0.20	0.07	0.16	0.03	0.24	0.05	0.02
H_2O	2.00	2.00	2.00	2.00	2.00	2.00	2.00	2.00	2.00	2.00	2.00	2.00
Total	96.72	96.31	96.05	97.56	96.95	97.37	97.93	99.62	99.84	97.86	98.93	98.85
Si	6.985	7.519	7.131	6.888	7.289	7.263	7.924	7.469	7.810	7.086	7.881	7.942
Al^{IV}	1.015	0.481	0.869	1.112	0.711	0.737	0.076	0.531	0.190	0.914	0.119	0.058
Al^{VI}	1.073	0.896	0.909	1.163	1.021	1.112	0.401	0.448	0.282	0.687	0.151	0.033
Ti	0.039	0.012	0.025	0.032	0.012	0.022	0.003	0.009	0.002	0.010	0.000	0.000
Cr	0.000	0.000	0.004	0.005	0.006	0.000	0.006	0.010	0.000	0.000	0.000	0.000
Fe^{2+}	2.120	1.444	1.948	2.226	1.524	1.691	1.601	0.627	0.510	1.539	1.039	1.125
Mg	1.883	2.657	2.193	1.708	2.480	2.209	2.869	4.048	4.337	2.951	3.890	3.908
Mn	0.037	0.024	0.025	0.012	0.026	0.027	0.037	0.031	0.015	0.030	0.030	0.024
Ca	1.114	1.418	1.276	1.121	1.456	1.223	1.859	1.677	1.743	1.458	1.848	1.942
Na	1.250	0.661	1.093	1.251	0.610	1.009	0.146	0.463	0.275	0.844	0.143	0.049
K	0.055	0.026	0.029	0.074	0.030	0.037	0.013	0.028	0.005	0.044	0.009	0.004

* *Combin unit (all other analyzed Ca-clinoamphiboles from Zermatt-Saas unit)*

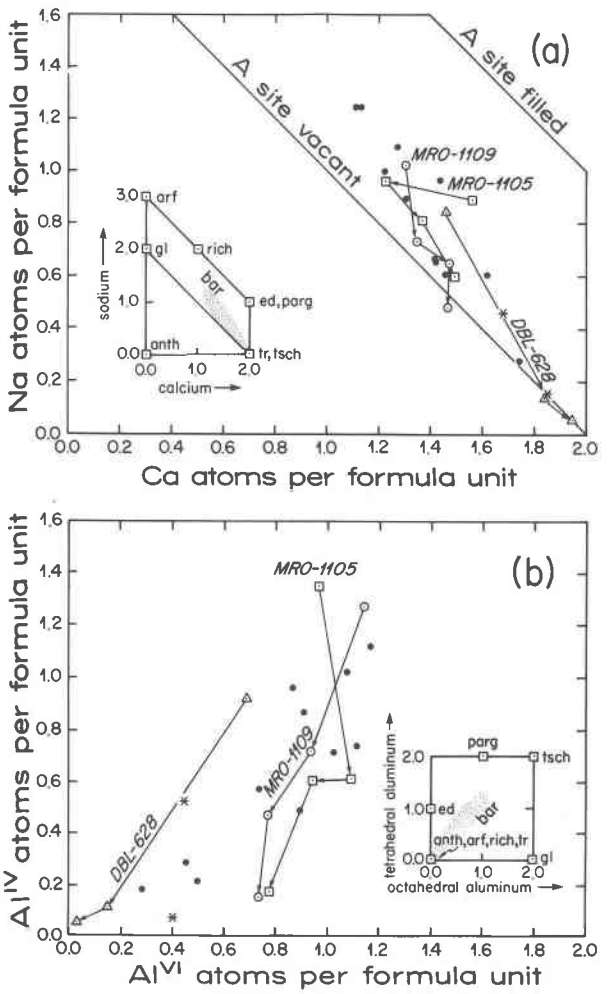

Fig. 7. Aspects of the chemical variations of Breuil–St. Jacques calcic amphiboles from eclogites and related rocks. Cation values are presented for 24 anions. Most specimens are homogeneous, but strongly-zoned Ca–amphiboles from samples MRO-1105 (open squares), MRO-1109 (open circles), and DBL-628 (open triangles) were also analyzed; arrows point towards later members of the series. (a) Sodium and calcium occupancy of M4 + A structural positions; (b) concentrations of aluminum in four- and six-coordinated sites. DBL-628 and the two starred samples are from the Combin unit, all others being from the Zermatt–Saas unit.

appropriate for barroisite–actinolite solid solutions. In general, analyzed Combin calcic amphiboles tend to be richer in Ca, poorer in Ti, Al^{IV}, Al^{VI}, and alkalis than the analogous phase from the Zermatt–Saas unit.

Epidote–clinozoisite

Analyses of 19 epidote-group minerals, including three core + rim pairs, are presented in Table 5. Specimens MRO-1783, DBL-510, DBL-515, and DBL-628 are from the Combin unit; all other analyzed epidotes are from the Zermatt–Saas unit. Cation totals based on one formula unit range from 7.998 to 8.028 and average 8.011, in excellent agreement with the theoretical value of 8.00. Potassium appears to be absent, but minor amounts of Ti, Cr, Mg, Mn, and Na are present, averaging 0.006, 0.001, 0.005, 0.009, and 0.001 respectively, based on 13 anions. Calcium and silicon contents are also quite uniform, with ranges of 1.893–1.984 and 2.869–2.904, close to the ideal formula values of 2.00 and 3.00 respectively.

The only major chemical variability appears to be in terms of ferric iron and aluminum contents. Values for the $Fe^{3+}/(Al^{VI} + Fe^{3+})$ ratio lie between the extremes 0.028 and 0.267, indicating compositions ranging between clinozoisite and pistacite. The four analyzed Combin samples are slightly more aluminous than counterparts from the Zermatt–Saas unit. Two of the three zoned samples, DBL-510 and DBL-547, exhibit indistinct iron depletion of the rims, whereas DBL-497 possesses a margin slightly enriched in ferric iron relative to the core. The inverted zoning of epidote (*i.e.*, Fe^{3+}-rich cores, Al-rich rims) is common within the region affected by the Lepontine recrystallization, extending from the Monte Rosa through the Piemonte ophiolite nappe between the Sesia and Ayas valleys; in some cases this inversion is accompanied by albitic plagioclase bordered by oligoclase (Dal Piaz, 1966).

White mica

Analyses of 12 white micas are listed in Table 6. Of this total, nine are paragonites; the remaining three are phengites, one of which, MRO-1783, is from the Combin unit. A pair of coexisting white micas was analyzed from samples DBL-409. Based on 12 anions, cation totals for paragonites and phengites range from 7.004–7.066 (average = 7.027) and 7.034–7.056 (average = 7.042), respectively, reasonably close to the theoretical dioctahedral value of 7.00. Other than aluminum, octahedrally-coordinated cations are present only in very minor concentrations in analyzed paragonites, whereas moderate amounts of these constituents characterize the phengites. Average abundances per formula unit for paragonite are: Ti = 0.003, Cr = 0.001, Fe^{2+} = 0.027, Mg = 0.021, and Mn = 0.001. Comparable values for phengite are: Ti = 0.009, Cr = 0.003; Fe^{2+} = 0.124, Mg = 0.272, and Mn = 0.001. Calcium, probably situated in the twelve-coordinated interlayer position, averages 0.013 in paragonites and 0.002 in phengites.

The Al^{VI}–Si and Na–K proportions are illustrated

in Figure 8. As evident from Figure 8a, the octahedrally-coordinated aluminum slightly exceeds 2.00 for sodic micas; moreover, the sum of six-fold cations for the three phengites (not shown) ranges from 2.106 to 2.117. Hence, all analyzed white micas have a slight cation excess over the stoichiometric dioctahedral value. This excess is balanced by a small charge deficiency in the interlayer position (see Fig. 8b). The maximum extent of Al^{VI}–Si and Na–K solid solution is shown by the coexisting paragonite + phengite pair of sample DBL-409. Based on K/(Na + K) ratios, their compositions are $Ms_{15}Pa_{85}$ and $Ms_{89}Pa_{11}$ respectively.

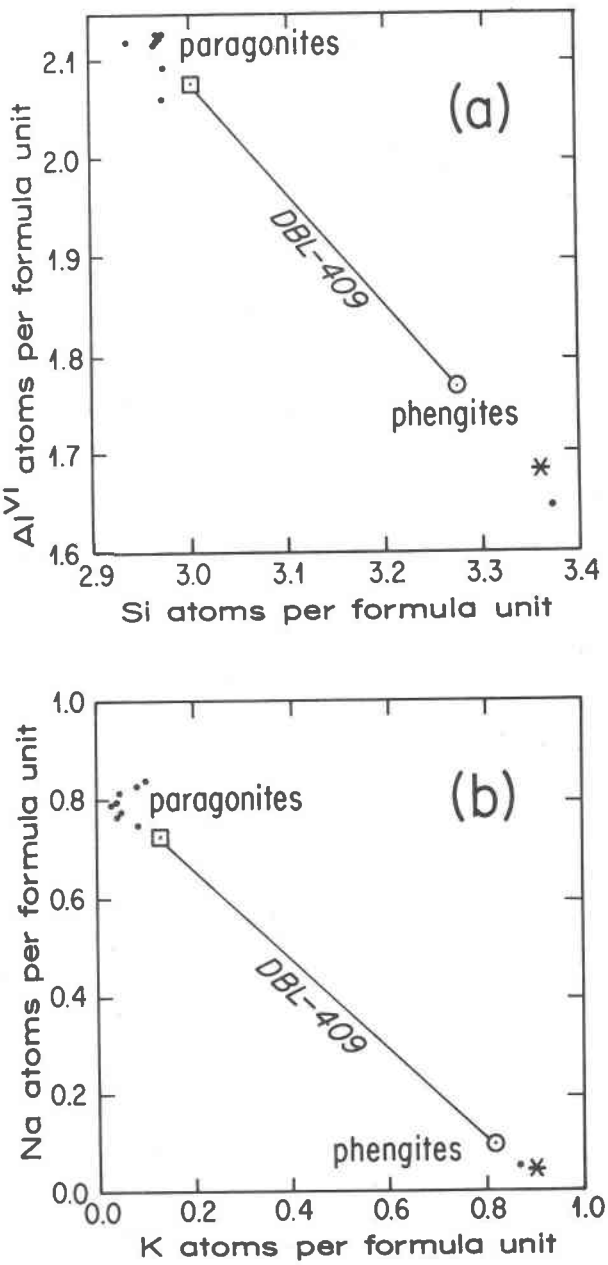

Fig. 8. Atomic proportions based on 12 anions of (a) Al^{VI} *vs.* Si, and of (b) Na *vs.* K for white micas from Breuil–St. Jacques eclogitic and other mafic rocks. The coexisting paragonite (open square) + phengite (open circle) pair analyzed from sample DBL-409 is also shown. The starred sample is from the Combin unit, all others being from the Zermatt–Saas unit.

Chlorite

Analyses of eight chlorites are presented in Table 7; of these eight, three (MRO-1783, DBL-510 and DBL-628) are from the Combin unit. Oxide totals are uniformly low, ranging from 92.27–99.64 weight percents. Such low totals may be partly a result of systematic underestimation of H_2O contents, but it can hardly account for the entire discrepancy. In spite of this problem, cation proportions appear to be quite reasonable. Based on 18 anions, cation totals range from 9.695 to 10.010 and average 9.797, approaching the ideal stoichiometric value of 10.00. With the exception of sample MRO-1783, which contains 0.017 Cr per formula unit, none of the chlorites possesses any chromium. The analyzed chlorites carry negligible potassium except for a single sample, DBL-510, which has 0.019 K per 18 anions. For all eight chlorites, other minor cations Ti, Mn, Ca, and Na are present in amounts averaging 0.004, 0.021, 0.004, and 0.003 respectively, based on one formula unit. The ratio of Al^{VI}/Al^{IV} ranges from 0.961 to 1.178 and averages 1.069, reflecting a simple clinochlore-type coupled substitution of $Al^{IV} + Al^{VI}$ for Si + Mg.

As is apparent from Figure 9, the eight analyzed chlorites are classified as ripidolites. Their iron–magnesium proportions seem to be chiefly a function of host-rock bulk composition. Their silicon contents are remarkably constant, ranging only from 2.613 to 2.768 per 18 anions. Figure 9 shows, however, a faint tendency for Combin-unit chlorites to be more siliceous than the analogous phase from the Zermatt–Saas unit.

Albite

Ten analyses of sodic plagioclase are presented in Table 8; four of these samples are from the Combin unit, the rest being Zermatt–Saas albites. Based on eight oxygens, cation totals range between 4.960–5.007 and average 4.984, in excellent agreement with the stoichiometric value of 5.00. With the exception of ferric iron, minor elements are present in negligible amounts. Averages per formula unit are: Ti, Cr, and Mg = 0.000; Fe^{3+} = 0.003; and Mn = 0.001. Based

Table 5. Electron microprobe analyses of epidote-clinozoisites from eclogitic parageneses, Breuil-St. Jacques area

Oxide	Sample Number									
	MRO-857	MRO-1109	MRO-1609	MRO-1611	MRO-1624r	MRO-1634	MRO-1756	MRO-1783*	DBL-379	DBL-409
SiO_2	36.26	38.51	38.23	37.42	37.17	37.26	37.62	38.09	37.89	38.16
Al_2O_3	28.31	29.84	30.78	29.50	26.02	27.94	30.00	31.47	28.81	30.72
TiO_2	0.09	0.08	0.13	0.08	0.07	0.08	0.16	0.18	0.08	0.21
Cr_2O_3	0.03	0.00	0.00	0.00	0.04	0.09	0.00	0.14	0.00	0.00
Fe_2O_3	8.52	9.34	7.66	8.66	14.07	11.22	8.58	6.31	10.28	7.66
MgO	0.11	0.04	0.05	0.04	0.02	0.07	0.03	0.03	0.04	0.06
MnO	0.04	0.11	0.07	0.05	0.25	0.20	0.16	0.42	0.09	0.03
CaO	23.40	23.91	23.46	23.57	22.95	22.86	23.53	23.77	23.45	23.56
Na_2O	0.00	0.00	0.01	0.00	0.00	0.01	0.00	0.00	0.00	0.00
K_2O	0.00	0.00	0.00	0.00	0.00	0.00	0.00	0.02	0.00	0.00
H_2O	2.00	2.00	2.00	2.00	2.00	2.00	2.00	2.00	2.00	2.00
Total	98.76	103.83	102.39	101.33	102.59	101.71	102.09	102.44	102.65	102.41
Si	2.869	2.896	2.895	2.880	2.878	2.880	2.872	2.880	2.891	2.890
Al^{IV}	0.131	0.104	0.105	0.120	0.122	0.120	0.128	0.120	0.109	0.110
Al^{VI}	2.509	2.540	2.642	2.555	2.253	2.425	2.572	2.684	2.482	2.632
Ti	0.005	0.004	0.008	0.004	0.004	0.005	0.009	0.010	0.005	0.012
Cr	0.002	0.000	0.000	0.000	0.003	0.005	0.000	0.009	0.000	0.000
Fe^{3+}	0.508	0.528	0.437	0.502	0.820	0.652	0.493	0.359	0.590	0.437
Mg	0.012	0.005	0.006	0.005	0.003	0.008	0.004	0.004	0.005	0.007
Mn	0.003	0.007	0.005	0.003	0.016	0.013	0.010	0.027	0.006	0.002
Ca	1.984	1.926	1.903	1.944	1.904	1.893	1.925	1.926	1.917	1.912
Na	0.000	0.000	0.001	0.000	0.000	0.002	0.000	0.000	0.000	0.000
K	0.000	0.000	0.000	0.000	0.000	0.000	0.000	0.002	0.000	0.000

r = rim
** Combin unit (all other analyzed epidote-clinozoisites from Zermatt-Saas unit)*

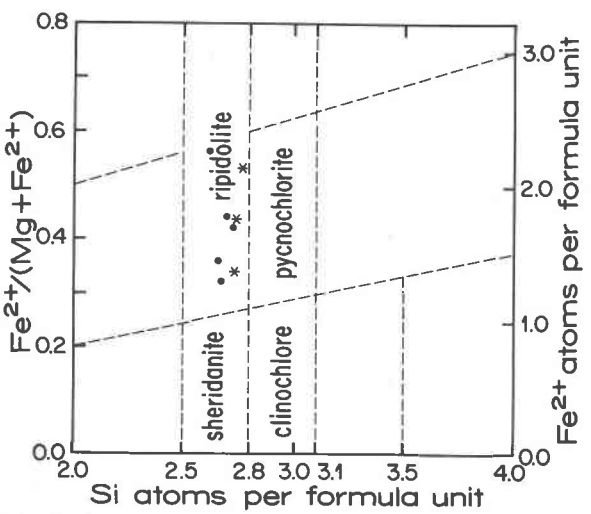

Fig. 9. Atomic proportions based on 18 anions of Breuil-St. Jacques chlorites from eclogitic and other mafic rocks. The classification employed is that of Hey (1954), but note that only a small portion of the chlorite diagram is illustrated. Starred samples are from the Combin unit, all others being from the Zermatt-Saas unit.

on eight oxygens, the Ca and K ranges are 0.002–0.018 and 0.001–0.003 respectively. The ten analyzed plagioclases are extremely albitic, possessing an average rather uniform composition of $Or_{0.2}Ab_{98.7}An_{1.1}$. No obvious chemical distinction between albites from the two zones is evident from Table 8.

Sphene

Analyses of sphenes from six different rocks, of which DBL-510 and DBL-515 are from the Combin unit, are listed in Table 9. Cation totals range from 3.014 to 3.033 and average 3.025 per five oxygens, in good agreement with the $CaTiSiO_5$ formula. Small but significant concentrations of aluminum and ferrous iron occur in these sphenes. Based on five oxygens, Al^{VI} ranges from 0.042 to 0.104, and Fe^{2+} from 0.005 to 0.012. None of the samples carry potassium, and Cr, Mg, Mn, and Na contents per formula unit only average 0.000, 0.001, 0.002 and 0.002 respectively. Major-element ranges also are very small: Ca = 0.989–1.004, Ti = 0.919–0.968, and Si = 0.988–

Table 5. (continued)

Oxide	Sample Number DBL-488	DBL-497c	DBL-497r	DBL-510c*	DBL-510r*	DBL-515*	DBL-547c	DBL-547r	DBL-628*
SiO_2	37.85	37.91	38.44	38.34	38.29	38.51	38.78	37.44	38.03
Al_2O_3	30.37	31.81	30.91	29.91	31.51	31.16	35.07	34.40	30.38
TiO_2	0.15	0.11	0.15	0.09	0.09	0.02	0.02	0.00	0.09
Cr_2O_3	0.04	0.00	0.00	0.00	0.00	0.00	0.00	0.00	0.00
Fe_2O_3	7.10	6.04	7.62	8.48	6.99	7.13	2.15	1.50	7.83
MgO	0.05	0.05	0.06	0.00	0.02	0.03	0.03	0.02	0.04
MnO	0.15	0.09	0.11	0.17	0.24	0.19	0.09	0.08	0.18
CaO	23.61	23.86	23.73	23.84	23.85	23.61	24.42	23.68	23.28
Na_2O	0.00	0.03	0.02	0.00	0.00	0.00	0.02	0.02	0.00
K_2O	0.00	0.00	0.00	0.00	0.00	0.00	0.00	0.02	0.00
H_2O	2.00	2.00	2.00	2.00	2.00	2.00	2.00	2.00	2.00
Total	101.31	101.90	103.05	102.82	102.99	102.64	102.58	99.15	101.83
Si	2.897	2.874	2.894	2.904	2.881	2.904	2.881	2.870	2.898
Al^{IV}	0.103	0.126	0.106	0.096	0.119	0.096	0.119	0.130	0.102
Al^{VI}	2.637	2.716	2.637	2.574	2.675	2.674	2.952	2.979	2.627
Ti	0.009	0.007	0.009	0.005	0.005	0.001	0.001	0.000	0.005
Cr	0.003	0.000	0.000	0.000	0.000	0.000	0.000	0.000	0.000
Fe^{3+}	0.409	0.345	0.432	0.483	0.396	0.402	0.120	0.087	0.449
Mg	0.006	0.006	0.007	0.000	0.002	0.004	0.003	0.002	0.005
Mn	0.009	0.006	0.007	0.011	0.015	0.012	0.006	0.005	0.011
Ca	1.936	1.939	1.914	1.935	1.923	1.908	1.944	1.945	1.901
Na	0.000	0.004	0.003	0.000	0.000	0.000	0.002	0.003	0.000
K	0.000	0.000	0.000	0.000	0.000	0.000	0.000	0.002	0.000

c = core; r = rim
** Combin unit (all other analyzed epidote-clinozoisites from Zermatt-Saas unit)*

1.001. Clearly, except for a minor aluminum substitution in octahedral sites, sphenes are essentially ideal stoichiometric phases; they display no compositional variation as a function of occurrence.

Physical conditions of metamorphism

The paragenetic sequence described from Breuil–St. Jacques eclogites and related rocks is remarkably similar to phase assemblages developed in eclogitic lithologies of Alpine age from other portions of the Western, Eastern, and Ligurian Alps. Physical conditions attending the formation and recrystallization of these metabasaltic rocks are difficult to evaluate because of the multivariance of the assemblages (*e.g.*, typical stable associations consist of three to six minerals in an 8–10 component system). However, several important reactions may be studied quantitatively for these rocks in an attempt to assess the *P–T* history reflected in the mineral paragenesis. Critical data are summarized in Figure 10. Implicit in this treatment is the assumption of local chemical equilibrium. This subject will be returned to in the next section.

Experimental and computational approaches to the disproportionation of ferrous iron and magnesium between coexisting garnet and Na–clinopyroxene as a function of the physical conditions of origin have been presented by Banno (1970), Råheim and Green (1974, 1975), and Ernst (1976) (see also Wood and Banno, 1973). The data of Tables 1 and 2 were employed to determine the equilibrium constant for this exchange reaction. K_D values[5] for Valtournanche and Ayas Valley garnet + omphacite pairs range from 12 to 31 and average 21 ($\sigma = \pm 6$). The spread of numerical values reflected in the high standard deviation indicates that little significance should be attached to the exact figures, except to note that ferrous iron is strongly concentrated in garnet relative to the clinopyroxene.

Of course, use of the data in Tables 1 and 2 in-

[5] *i.e.*, the ratio $(Fe^{2+}/Mg)_{garnet}/(Fe^{2+}/Mg)_{clinopyroxene}$.

Table 6. Electron microprobe analyses of white micas from eclogitic parageneses, Breuil–St. Jacques area

Oxide	Sample Number											
	MRO-1609	MRO-1611	MRO-1624	MRO-1634	MRO-1756	MRO-1783*	DBL-379	DBL-409	DBL-409'	DBL-488	DBL-497	DBL-547
SiO_2	46.06	46.05	49.62	45.78	44.82	50.25	45.74	46.61	48.96	46.58	46.72	46.02
Al_2O_3	41.52	41.58	28.46	40.81	39.56	29.50	41.36	40.47	31.65	41.96	42.17	42.36
TiO_2	0.04	0.02	0.24	0.07	0.08	0.12	0.04	0.09	0.19	0.09	0.07	0.05
Cr_2O_3	0.00	0.00	0.04	0.08	0.00	0.04	0.03	0.00	0.07	0.04	0.04	0.00
FeO	0.39	0.67	2.64	0.76	0.36	1.80	0.38	0.91	2.15	0.29	0.49	0.27
MgO	0.16	0.10	2.88	0.26	0.42	3.09	0.13	0.37	2.16	0.21	0.20	0.11
MnO	0.01	0.00	0.00	0.00	0.00	0.04	0.00	0.00	0.00	0.00	0.05	0.07
CaO	0.14	0.19	0.02	0.12	0.15	0.02	0.18	0.12	0.02	0.16	0.19	0.36
Na_2O	6.40	6.16	0.42	5.96	6.45	0.33	6.47	5.76	0.75	6.25	6.41	6.78
K_2O	0.52	0.59	10.04	1.06	1.04	10.61	0.59	1.61	9.63	0.66	0.51	0.63
H_2O	4.00	4.00	4.00	4.00	4.00	4.00	4.00	4.00	4.00	4.00	4.00	4.00
Total	99.24	99.37	98.36	98.90	96.87	99.81	98.93	99.94	99.58	100.24	100.85	100.65
Si	2.969	2.967	3.371	2.972	2.971	3.360	2.961	3.003	3.274	2.972	2.967	2.935
Al^{IV}	1.031	1.033	0.629	1.028	1.029	0.640	1.039	0.997	0.726	1.028	1.033	1.065
Al^{VI}	2.123	2.124	1.649	2.094	2.061	1.685	2.116	2.075	1.768	2.127	2.123	2.119
Ti	0.002	0.001	0.012	0.003	0.004	0.006	0.002	0.005	0.009	0.004	0.004	0.003
Cr	0.000	0.000	0.003	0.004	0.000	0.003	0.002	0.000	0.004	0.002	0.002	0.000
Fe^{2+}	0.021	0.036	0.150	0.042	0.020	0.101	0.021	0.049	0.121	0.016	0.026	0.015
Mg	0.015	0.010	0.292	0.025	0.041	0.308	0.013	0.035	0.215	0.020	0.019	0.011
Mn	0.005	0.000	0.000	0.000	0.000	0.003	0.000	0.000	0.000	0.000	0.003	0.004
Ca	0.010	0.014	0.002	0.009	0.011	0.002	0.012	0.009	0.002	0.011	0.013	0.025
Na	0.799	0.770	0.055	0.750	0.829	0.043	0.813	0.720	0.097	0.773	0.790	0.838
K	0.043	0.049	0.871	0.088	0.088	0.905	0.049	0.133	0.821	0.054	0.041	0.051

* *Combin unit (all other analyzed white micas from Zermatt-Saas unit)*

volves the assumption that all the iron is divalent in garnet, whereas the coexisting omphacite carries equal amounts of Fe^{2+} and Fe^{3+}. Judging from the garnet cation proportions—especially the very high Al^{VI} contents—the assumption seems reasonable. However, instead of assuming a fixed ratio, several different computations may be employed to determine the Fe^{3+}/Fe^{2+} ratios in the associated clinopyroxene. For instance, ferrous iron in omphacite has been calculated (a) letting $Fe^{2+} = Fe_{total} - Fe^{3+} = Fe_{total} - (Na - Al^{VI})$. Alternatively, ferrous iron was determined (b) letting $Fe^{2+} = Ca - Mg - Mn$. Both methods ignore small amounts of $CaAl_2SiO_6$ end-member, but inasmuch as Al^{IV} values average only 0.005 per six oxygens for the 10 analyzed clinopyroxenes coexisting with garnet, this would be a trivial correction. Computational schemes (a) and (b) yield different Fe^{3+}/Fe^{2+} ratios, reflecting small departures of the omphacites from ideal stoichiometry and minor impurities such as Ti and Cr; such variations are magnified because total iron contents in the Valtournanche and Val d'Ayas clinopyroxenes are fairly low. Mean K_D values utilizing methods (a) and (b) are 27 ± 12 and 17 ± 7 respectively, but the ranges are greater than for the case assuming equal amounts of Fe^{3+} and Fe^{2+}. Furthermore, it is not clear which of these two calculations provides the more reasonable distribution constants, and an average of (a) + (b) yields a mean K_D indistinguishable from that obtained employing the initial assumption. Accordingly, the Fe^{3+}/Fe^{2+} ratio of unity originally assumed for the omphacites is preferred.

If we accept the transition boundary between garnet granulite and eclogite published by Green and Ringwood (1967, 1972) (see also Ito and Kennedy, 1971), and utilize the experimentally-determined values for K_D of Råheim and Green (1974), it is clear that the average partition values computed for the Breuil–St. Jacques eclogites require lithostatic pressures exceeding 8–10 kbar during formation. The K_D value of 21 closely matches the range of Japanese and Californian blueschist-belt eclogite occurrences (type C of Coleman *et al.*, 1965) of 20–23 measured by Banno (1970) and Ernst *et al.* (1970) respectively. For

Table 7. Electron microprobe analyses of chlorites from eclogitic parageneses, Breuil–St. Jacques area

Oxide	Sample Number							
	MRO-1624	MRO-1634	MRO-1756	MRO-1783*	DBL-409	DBL-488	DBL-510*	DBL-628*
SiO_2	24.54	25.08	26.10	26.39	25.86	26.32	26.49	27.34
Al_2O_3	21.67	21.72	21.28	22.53	23.38	22.19	21.57	21.01
TiO_2	0.09	0.06	0.03	0.05	0.05	0.08	0.00	0.00
Cr_2O_3	0.00	0.00	0.00	0.20	0.00	0.00	0.00	0.00
FeO	25.36	14.55	20.43	20.14	16.66	19.48	24.22	16.12
MgO	13.46	18.67	18.11	15.76	18.65	17.03	13.62	22.84
MnO	0.22	0.16	0.26	0.32	0.07	0.21	0.40	0.26
CaO	0.02	0.00	0.02	0.08	0.02	0.02	0.08	0.06
Na_2O	0.02	0.04	0.02	0.00	0.00	0.00	0.01	0.00
K_2O	0.01	0.00	0.01	0.01	0.00	0.00	0.14	0.00
H_2O	12.00	12.00	12.00	12.00	12.00	12.00	12.00	12.00
Total	97.38	92.27	98.26	97.48	96.69	97.33	98.52	99.64
Si	2.613	2.674	2.697	2.736	2.660	2.725	2.768	2.739
Al^{IV}	1.387	1.326	1.303	1.264	1.340	1.275	1.232	1.261
Al^{VI}	1.333	1.403	1.288	1.489	1.496	1.433	1.425	1.220
Ti	0.007	0.005	0.002	0.004	0.004	0.006	0.000	0.000
Cr	0.000	0.000	0.000	0.017	0.000	0.000	0.000	0.000
Fe^{2+}	2.259	1.298	1.765	1.746	1.433	1.687	2.117	1.351
Mg	2.135	2.967	2.789	2.435	2.859	2.627	2.122	3.410
Mn	0.020	0.014	0.023	0.028	0.006	0.018	0.035	0.022
Ca	0.002	0.000	0.002	0.009	0.002	0.002	0.009	0.007
Na	0.005	0.008	0.004	0.000	0.000	0.000	0.002	0.000
K	0.002	0.000	0.002	0.002	0.000	0.000	0.019	0.000

** Combin unit (all other analyzed chlorites from Zermatt-Saas unit)*

these, and similar parageneses such as those from Valtournanche and Val d'Ayas, temperatures near 500°C have been determined by Taylor and Coleman (1968) (see also Ghent and Coleman, 1973) employing oxygen-isotope geothermometry. Closely similar values, averaging 540°C, have been determined using oxygen-isotope geothermometry by Desmons and O'Neil (1977) for eclogitic and blueschistic mineral assemblages within the Austroalpine continental crust of the Sesia–Lanzo nappe; this sheet apparently overrode and now tectonically overlies the Piemonte ophiolite nappe (Compagnoni *et al.*, 1975). The thermal values obtained from O^{18}/O^{16} data correspond closely to temperatures determined utilizing Fe^{2+}–Mg partitioning between coexisting garnets and omphacites on these same rocks by Desmons and Ghent (1977).

Using Råheim and Green's *P–T* grid for Fe^{2+}–Mg fractionation in garnet + omphacite pairs, a K_D value of 21, and assigning total pressures of 8, 10, and 12 kbar to the formation of the Breuil–St. Jacques eclogites, the indicated temperatures are 455, 466, 476°C respectively (Fig. 10a). Thus the original assumption of equal amounts of ferrous and ferric iron in Na–clinopyroxene appears to provide computed physical conditions of origin of approximately 470 ± 50°C and 10 ± 2 kbar—comparable to *P–T* conditions calculated for similar type-C eclogites from elsewhere.

Based on overall mineral assemblages and phase compositions, Chinner and Dixon (1973) arrived at conditions for eclogitic recrystallization of the Allalin metagabbro from Zermatt–Saas Fee of 15 kbar, 570–700°C, whereas for the Etiral–Levaz metagabbro of the lower Valtournanche Kienast (1976) estimated the conditions of Alpine high-pressure metamorphism as $P \geq 10$ kbar, $T = 500$–600°C. These temperature estimates somewhat exceed those of the present investigation and in general seem a trifle high, judging by the observation that such eclogitic rocks—and those of the Breuil–St. Jacques area as well—have been transformed to blueschists and albite + barroisitic amphibole schists rather than to high-rank amphibolites.

Table 8. Electron microprobe analyses of albites from eclogitic parageneses, Breuil–St. Jacques area

Oxide	Sample Number									
	MRO-1109	MRO-1624	MRO-1756	MRO-1783*	DBL-409	DBL-488	DBL-510*	DBL-515*	DBL-547	DBL-628*
SiO_2	68.70	67.84	66.98	68.02	67.53	67.54	68.39	67.92	68.33	67.44
Al_2O_3	20.23	19.93	19.84	19.74	20.04	20.00	20.40	19.70	19.82	19.55
TiO_2	0.02	0.00	0.00	0.00	0.03	0.00	0.00	0.00	0.00	0.00
Cr_2O_3	0.00	0.00	0.00	0.00	0.00	0.00	0.00	0.00	0.00	0.00
Fe_2O_3	0.05	0.21	0.11	0.10	0.09	0.08	0.08	0.06	0.07	0.13
MgO	0.00	0.00	0.00	0.00	0.00	0.00	0.00	0.00	0.00	0.00
MnO	0.02	0.00	0.01	0.00	0.00	0.00	0.06	0.06	0.06	0.06
CaO	0.23	0.18	0.39	0.05	0.29	0.22	0.19	0.39	0.14	0.21
Na_2O	11.14	11.03	11.45	11.35	11.35	11.07	10.89	11.44	11.43	11.31
K_2O	0.03	0.04	0.03	0.05	0.02	0.04	0.06	0.06	0.03	0.03
Total	100.43	99.22	98.81	99.32	99.36	98.95	100.08	99.62	99.88	98.73
Si	2.982	2.981	2.965	2.987	2.969	2.977	2.977	2.980	2.986	2.983
Al^{IV}	1.035	1.032	1.035	1.022	1.039	1.039	1.047	1.019	1.021	1.019
Ti	0.001	0.000	0.000	0.000	0.001	0.000	0.000	0.000	0.000	0.000
Cr	0.000	0.000	0.000	0.000	0.000	0.000	0.000	0.000	0.000	0.000
Fe^{3+}	0.002	0.007	0.004	0.003	0.003	0.003	0.003	0.002	0.002	0.004
Mg	0.000	0.000	0.000	0.000	0.000	0.000	0.000	0.000	0.000	0.000
Mn	0.001	0.000	0.000	0.000	0.000	0.000	0.002	0.002	0.002	0.002
Ca	0.011	0.008	0.018	0.002	0.014	0.010	0.009	0.018	0.007	0.010
Na	0.937	0.940	0.983	0.967	0.968	0.946	0.919	0.973	0.969	0.970
K	0.002	0.002	0.002	0.003	0.001	0.002	0.003	0.003	0.002	0.002

* *Combin unit (all other analyzed albites from Zermatt-Saas unit)*

Table 9. Electron microprobe analyses of sphenes from eclogitic parageneses, Breuil–St. Jacques area

Oxide	Sample Number					
	MRO-1609	DBL-409	DBL-488	DBL-497	DBL-510*	DBL-515*
SiO_2	30.51	30.43	29.94	30.79	30.78	30.52
Al_2O_3	2.69	2.41	1.84	2.06	1.54	1.26
TiO_2	37.23	38.05	38.38	38.22	39.73	39.47
Cr_2O_3	0.00	0.00	0.00	0.00	0.00	0.00
FeO	0.45	0.39	0.24	0.30	0.18	0.22
MgO	0.02	0.01	0.00	0.00	0.00	0.03
MnO	0.05	0.00	0.03	0.07	0.12	0.08
CaO	28.14	28.78	28.34	28.85	28.81	28.43
Na_2O	0.03	0.05	0.03	0.01	0.01	0.01
K_2O	0.00	0.00	0.00	0.00	0.00	0.00
Total	99.12	100.11	98.81	100.30	101.18	100.03
Si	1.001	0.991	0.988	1.000	0.992	0.994
Al^{IV}	0.000	0.009	0.012	0.000	0.008	0.006
Al^{VI}	0.104	0.083	0.060	0.079	0.051	0.042
Ti	0.919	0.932	0.953	0.934	0.963	0.968
Cr	0.000	0.000	0.000	0.000	0.000	0.000
Fe^{2+}	0.012	0.010	0.007	0.008	0.005	0.006
Mg	0.001	0.001	0.000	0.000	0.000	0.002
Mn	0.001	0.000	0.001	0.002	0.003	0.002
Ca	0.989	1.004	1.002	1.004	0.995	0.993
Na	0.002	0.003	0.002	0.001	0.001	0.001
K	0.000	0.000	0.000	0.000	0.000	0.000

* *Combin unit (all other analyzed sphenes from Zermatt-Saas unit)*

At pressures greater than a few tens of bars and less than about 25 kbar, experimental and theoretical studies of basaltic compositions have shown that unless H_2O is absent, or at least the activity of H_2O achieves a very low value, amphibolitic assemblages totally replace eclogitic compatibilities under equilibrium conditions. Therefore, it seems certain that a_{H_2O} was very low during production of the eclogites from the Breuil–St. Jacques area. However, these rocks and nearby units in the Western Alps display evidence of succeeding glaucophane–schist-facies assemblages, including lawsonite and sphene rather than calcite + quartz + rutile; accordingly, judging from experimental and theoretical studies (Schuiling and Vink, 1967; Ernst, 1972; Nitsch, 1972, 1974; Hunt and Kerrick, 1977), post-eclogitic recrystallization was characterized by somewhat increased values for a_{H_2O} and low to extremely low a_{CO_2}.

Transformation (retrogression) of the Valtournanche and Val d'Ayas eclogites to blueschists therefore undoubtedly accompanied the introduction of aqueous fluids. Maresch (1977) has shown that earlier phase-equilibrium experiments on the $Na_2Mg_3Al_2Si_8O_{22}(OH)_2$ composition have not produced true glaucophane; his results suggest that a

relatively magnesian natural glaucophane is stable below approximately 350°C only above a minimum pressure of four kbar ($\approx P_{H_2O}$), and below 550°C at 10 kbar. Apparently, in a rock of its own bulk composition, this sodic amphibole would break down above 450°C at, say, 7 kbar; accordingly, glaucophane schists clearly could not be stable at comparable temperatures and even lower pressures (Fig. 10b). High bulk-rock Fe/Mg ratios would tend to reduce this threshold pressure to some extent.

Greenschistic and epidote–amphibolitic assemblages such as are ubiquitous as late-stage compatibilities in the upper Valtournanche and Ayas Valley occurrences appear to be stable, even at low pressure of about two or three kbar P_{fluid} ($\approx P_{H_2O}$), up to approximately 475°C according to the work of Liou (1973) and Liou *et al.* (1974). The single pair of coexisting white micas from near Breuil, sample DBL-409, provides another check on prasinitic *P–T* conditions. According to the 2 kbar data of Eugster *et al.* (1972), the phengite ($Ms_{89}Par_{11}$) would have equilibrated at about 390°C; however, the coexisting paragonite ($Ms_{15}Par_{85}$) contains rather large amounts of Ms, hence the solvus composition provides an unacceptable apparent temperature of crystallization of approximately 680°C. If its composition lies along the 2 kbar chemical spinodal, the paragonite could have formed metastably at around 425°C according to the curves of Eugster *et al.*, but there seems to be no *a priori* reason to suspect that the K-rich white mica crystallized under equilibrium conditions along the solvus whereas the coexisting Na-rich white mica crystallized metastably along the chemical spinodal. More probably, undetected submicroscopic lamellae of Ms are regularly interlayered with the paragonite. It must also be added that, for K-rich white micas, the effect of solid solution towards phengite on the Ms–Pa solvus is not well known. In summary, the best but somewhat unsatisfactory guess is that greenschist physical conditions during white-mica formation involved temperatures approaching 400°C, with pressure ($P_{fluid} \approx P_{total}$) on the order of roughly 3 kbar (Fig. 10b).

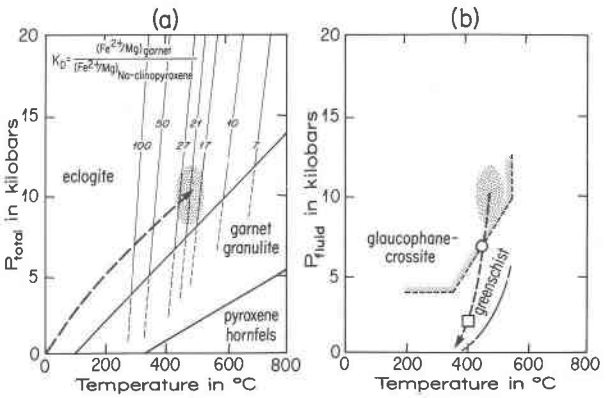

Fig. 10. Physical conditions of metamorphism for Breuil–St. Jacques eclogites and related rocks as deduced from mineral assemblages, compositions of coexisting phases, and experimentally-determined heterogeneous equilibria. (a) Prograde *P–T* trajectory showing eclogitic culmination. Field boundaries for dry metabasaltic rocks are after Green and Ringwood (1967, 1972), Fe–Mg partitioning between garnet and clinopyroxene pairs after Råheim and Green (1974, 1975). (b) Retrograde *P–T* trajectory showing observed upper Valtournanche and Val d'Ayas sequence, from eclogitic (stippled pattern) through glaucophanic (open circle) to final micaceous prasinitic stage (square). The stability field for iron-poor glaucophane in a rock of its own bulk composition is shown after Maresch (1977), the thermal stability limit for greenschists is after Liou *et al.* (1974) and represents the minimum pressure at which this amphibole could have formed, and the apparent temperature of equilibration of phengite associated with paragonite (sample DBL-409) is after Eugster *et al.* (1972), assuming a total pressure of about 2 kbar.

Approach to equilibrium

The preceding discussion demonstrates that, although the observed paragenetic relationships seem to reflect an orderly progressive change in physical conditions attending the various stages of metamorphism, the several assemblages may not have been in chemical equilibrium during or subsequent to their formation. An attempt was made to avoid analysis of zoned phases—clear evidence of disequilibrium. However, the distribution of elements such as Fe^{2+} and Mg (or Fe^{3+} and Al) between competing minerals (such as garnet + clinopyroxene pairs already discussed) provides another measure of the closeness of approach to equilibrium. The general theory of element partitioning was elucidated by Ramberg and deVore (1951); for a recent summary see Ernst (1976). The distribution of Fe, Mg, and Al between pairs of coexisting post-eclogitic phases is presented in Figure 11. Isofractionation lines of +45° slope have been added as an aid in visualization of the departures of the data from ideal ion-for-ion partitioning.

Figure 11a shows the fractionation of Fe^{2+} and Mg between omphacites and (early) glaucophane cores. Inasmuch as half of the total iron has been arbitrarily assigned a divalent state in both minerals, this diagram qualitatively shows the partitioning of total iron between the two phases as well. The equilibrium constant, K_D, $(Fe^{2+}/Mg)_{cpx}/(Fe^{2+}/Mg)_{glauc}$, averages 1.6 with a standard deviation of 0.3, hence iron is slightly enriched in the omphacite relative to coexisting sodic amphibole. The data are compatible with a fairly close approach to chemical equilibrium.

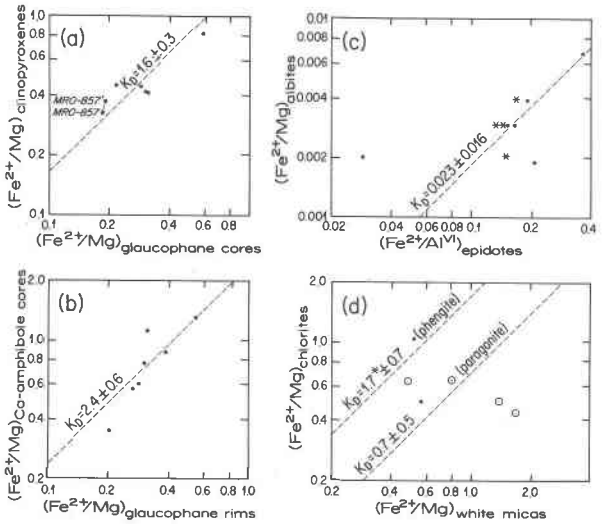

Fig. 11. Distribution of Fe, Mg, and Al between competing pairs of phases from Breuil–St. Jacques post-eclogitic schists. Log-log scales are employed for ordinates and abscissas; note different values for origins in all four diagrams. Black dots and open circles (= paragonites) indicate compositions of phases from the Zermatt–Saas unit, stars indicate Combin minerals. (a), (b), and (c) display fairly close approaches to equilibrium for omphacite + glaucophane, Ca–amphibole + glaucophane, and albite + epidote pairs respectively. (d) shows apparent nonsystematic partitioning of Fe^{2+} and Mg between coexisting layer silicates.

The distribution of these same elements between the (early) cores of calcic amphibole and the (late) rims of sodic amphibole is illustrated in Figure 11b. Again, a relatively close approach to chemical equilibrium is apparent, with $K_D = 2.4 \pm 0.6$, showing that hornblende markedly concentrates ferrous iron compared to the more magnesian glaucophane. Of course, it must be noted that all iron has been regarded as ferrous in the Ca–amphibole (an overestimation), whereas only half of the Fe was assigned a divalent state in the Na–amphibole (an underestimation); hence the derived K_D is probably too high.

The distribution of Fe^{3+} and Al between octahedral sites in epidote and tetrahedral sites in sodic plagioclase is presented in Figure 11c. Iron is very strongly concentrated in epidote relative to the much more aluminous albite, as reflected in the K_D, 0.023 ± 0.016. Although the data exhibit moderate scatter, this probably reflects the minor amounts of ferric iron in plagioclase—hence large percentage analytical error—rather than a nonsystematic fractionation of these two components. There appears to be no correlation between K_D and occurrence in the Zermatt–Saas *vs.* the Combin units.

The partitioning of Fe^{2+} and Mg between coexisting white micas and chlorite is shown in Figure 11d. Although analyzed phases within a single specimen seem to be homogeneous, there is no indication that the Fe/Mg ratio in white micas varies sympathetically with $(Fe^{2+}/Mg)_{chl}$. For the three potassic micas, including one Combin specimen, K_D averages 1.7 ± 0.7; for the four sodic micas, K_D averages 0.7 ± 0.5. Compared to magnesium, ferrous iron evidently is concentrated in chlorite with respect to phengite, but in paragonite relative to chlorite. Sample DBL-409 contains both white micas and, as anticipated from the above, $K_D\ (Fe^{2+}/Mg)_{par}/(Fe^{2+}/Mg)_{ms}$ is 2.5, thus paragonite is enriched in iron/magnesium compared to phengite.

We may tentatively conclude from the element-partitioning data that in the earlier higher-grade stages of post-eclogitic recrystallization a moderately close approach to chemical equilibrium was achieved. In contrast, the production of layer silicates—especially white micas—probably took place either over a broad range of P and T or under disequilibrium conditions.

Discussion

Experimental data for the systems discussed, as well as prograde and retrograde metamorphic P–T trajectories for the Breuil–St. Jacques paragenesis, are illustrated in Figure 10. Evidently the prograde path (Fig. 10a), represented exclusively by the metamorphic maximum—the eclogitic assemblage of the Zermatt–Saas unit—reflects a typical subduction zone metamorphism (Ernst, 1975), whereas retrogression (Fig. 10b) may have involved virtually an adiabatic rise towards the surface, *i.e.,* decompression recrystallization (Ernst, 1976). It must be admitted that the P–T paths are not well constrained by the mineralogic and chemical data, but they are compatible with them and with the known structure of the region and inferred geologic history (Dal Piaz and Ernst, in press). Almost all lithologic materials are poor thermal conductors, hence the illustrated P–T trajectories appear to be a consequence of the hypothesized rapid descent of the subducted ophiolitic section, followed by detachment from the downgoing lithospheric slab and buoyant return to shallower depths. If the original rocks had been altered, weathered, and hydrated through previous interactions with sea water and/or hydrothermal solutions, such volatile constituents must have been rather efficiently driven off during subduction, for the eclogitic culmination could only have been produced in an essentially anhydrous environment. The more or less adia-

batic return subsequent to decoupling probably involved the introduction of crustal aqueous fluids, hence the activity of H_2O seemingly would have increased as the detached high-pressure rocks approached the Earth's surface. The source of these fluids is unclear, but might have included the underlying subducted Pennine (Monte Rosa) continental crust. Figure 10a illustrates the Early Alpine high-pressure event, whereas relationships presented in Figure 10b perhaps are correlatable at least in part with a stage of the Lepontine thermal event (Hunziker, 1969, 1970, 1974; Bocquet *et al.*, 1974; Delaloye and Desmons, 1976).

These considerations indicate that in Early Alpine time the Zermatt–Saas unit underwent relatively high-pressure metamorphism, followed by Lepontine production of greenschists; on the other hand, the Combin unit recrystallized chiefly to prasinites under late-stage *P–T* conditions. Published bulk rock analyses (Dal Piaz and Ernst, in press) show that dissimilar parageneses in the two units are not a function of major differences in chemistry. Geologic and paragenetic contrasts support the idea that the Zermatt–Saas and Combin units were independent neighboring tectonic slices which were subducted to greater and lesser depths respectively. Their later juxtaposition presumably reflects continued but complex structural imbrication accompanying the final suturing of remnants of Mesozoic Tethys during continental collision (Dal Piaz *et al.*, 1972; Dal Piaz and Ernst, in press).

The high-pressure prograde path represented by the eclogitic culmination (stage A) in the Zermatt–Saas unit is characteristic of subduction zone metamorphism. In contrast, the retrograde *P–T* trajectory reflected by the glaucophanic → barroisitic → actinolitic sequence of both tectonic portions of the Piemonte ophiolite nappe probably reflects gradual unloading at nearly constant temperature; this latter recrystallization (stages B and C) evidently accompanied buoyant return of the subducted complex towards the surface after its detachment from the downgoing lithospheric slab. At least part of the greenschist-facies overprinting is connected with the Lepontine metamorphic event, which may be a consequence of post-collisional thermal reequilibration of the pile of nappes (Niggli, 1970), developing under conditions involving renewed compression.

Acknowledgments

This collaborative study was initiated while the first author held a Guggenheim Memorial Fellowship at the Eidgenössische Technische Hochschule, Zürich, and was completed at both the University of California, Los Angeles, and Università di Padova. Financial support was also provided by a U.S.–Italy Cooperative Project through the auspices of the National Science Foundation (EAR 77-10649) and the CNR (Centro di Studio per i problemi dell'orogeno delle Alpi occidentali, Torino). The manuscript benefited from constructive reviews by E. D. Ghent (University of Calgary), D. H. Green (University of Tasmania), and Volkmar Trommsdorff (Eidgenössische Technische Hochschule, Zürich). The authors thank the above institutions and reviewers for support and help.

References

Banno, S. (1970) Classification of eclogites in terms of physical conditions of their origin. *Phys. Earth Planet. Interiors, 3,* 405–431.

Bearth, P. (1953) Geologischer Atlas der Schweiz 1:25,000, Blatt Zermatt, mit Erläuterungen. *Schweiz. Geol. Kommission,* Bern.

——— (1967) Die Ophiolithe der Zone von Zermatt–Saas Fee. *Beitr. Geol. Karte der Schweiz, Neue Folge, 132.*

——— (1973) Gesteins- und Mineralparagenesen aus den Ophiolithen von Zermatt. *Schweiz. Mineral. Petrogr. Mitt., 53,* 299–334.

——— (1976) Zur Gliederung der Bündnerschiefer in der region von Zermatt. *Eclogae geol. Helv., 69,* 149–161.

Bocquet, J., M. Delaloye, J. C. Hunziker and D. Krummenacher (1974) K–Ar and Rb–Sr dating of blue amphiboles, micas and associated minerals from the Western Alps. *Contrib. Mineral. Petrol., 47,* 7–26.

Chinner, G. A. and J. E. Dixon (1973) Some high-pressure parageneses of the Allalin Gabbro, Valais, Switzerland. *J. Petrol., 14,* 185–202.

Coleman, R. G., D. E. Lee, L. B. Beatty and W. W. Brannock (1965) Eclogites and eclogites: their differences and similarities. *Geol. Soc. Am. Bull., 76,* 483–508.

Compagnoni, R., G. V. Dal Piaz, J. C. Hunziker, G. Gosso, B. Lombardo and P. F. Williams (1975) The Sesia–Lanzo zone, a slice of continental crust with Alpine high pressure–low temperature assemblages in the Western Italian Alps. *Rend. Soc. Ital. Mineral. Petrol., 33,* 1977, 281–334.

Dal Piaz, G. V. (1966) Gneiss ghiandoni, marmi ed anfiboliti antiche del ricoprimento Monte Rosa nell'alta Valle d'Ayas. *Boll. Soc. Geol. Ital., 85,* 103–132.

———, Gp. Devecchi and G. Mezzacasa (in press) Geochemistry of ophiolites, metavolcanics and metagabbros from the Ayas Valley and Valtournanche, the Western Alps. *Mem. Ist. Geol. Mineral., Univ. Padova.*

——— and W. G. Ernst (in press) Areal geology and petrology of the Piemonte ophiolite nappe, Breuil-St. Jacques area, Italian Western Alps. *Tectonophysics, 47.*

———, J. C. Hunziker and G. Martinotti (1972) La Zona Sesia–Lanzo e l'evoluzione tettonico–metamorfica delle Alpi nordoccidentali interne. *Mem. Soc. Geol. Ital., 11,* 433–466.

Delaloye, M. and J. Desmons (1976) K–Ar radiometric age determinations of white micas from the Piedmont zone, French-Italian Western Alps. *Contrib. Mineral. Petrol., 57,* 297–307.

Desmons, J. and D. Ghent (1977) Chemistry, zonation and distribution coefficients of elements in eclogitic minerals from the northeastern Sesia zone (abstr.). *Rend. Soc. Ital. Mineral. Petrol., 33,* 440–441.

——— and J. R. O'Neil (1977) Stable isotope measurements on minerals from eclogites and other rocks from the north-eastern Sesia zone (abstr.). *Rend. Soc. It. Mineral. Petrol., 33,* 1977, 440.

Dewey, J. F., W. G. Pitman, W. B. F. Ryan, and J. Bonnin (1973) Plate tectonics and the evolution of the Alpine System. *Geol. Soc. Am. Bull., 84,* 3137–3180.

Ernst, W. G. (1971) Metamorphic zonations on presumably subducted lithospheric plates from Japan, California and the Alps. *Contrib. Mineral. Petrol., 34,* 43–59.

——— (1972) CO_2-poor composition of the fluid attending Franciscan and Sanbagawa low-grade metamorphism. *Geochim. Cosmochim. Acta, 36,* 497–504.

——— (1973) Interpretative synthesis of metamorphism in the Alps. *Geol. Soc. Am. Bull., 84,* 2053–2078.

———, Ed. (1975) *Subduction zone metamorphism.* Dowden, Hutchinson and Ross, Stroudsburg, Pennsylvania.

——— (1976) Mineral chemistry of eclogites and related rocks from the Voltri Group, western Liguria, Italy. *Schweiz. Mineral. Petrogr., Mitt., 56,* 293–343.

———, Y. Seki, H. Onuki and M. C. Gilbert (1970) Comparative study of low-grade metamorphism in the California Coast Ranges and the Outer Metamorphic Belt of Japan. *Geol. Soc. Am. Mem. 124.*

Eugster, H. P., A. L. Albee, A. E. Bence, J. B. Thompson, Jr. and D. R. Waldbaum (1972) The two-phase region and excess mixing properties of paragonite–muscovite crystalline solutions. *J. Petrol., 13,* 147–179.

Franchi, S. (1898) Sull'età mesozoica della Zona delle Pietre Verdi nelle Alpi Occidentali. *Boll. R. Comit. Geol. Ital., 29,* 173–247 and 325–482.

Fry, N. and W. S. Fyfe (1971) On the significance of the eclogite facies in Alpine metamorphism. *Verh. Geol. Bundesanst., Wien, 2,* 257–265.

Ghent, E. D., and R. G. Coleman (1973) Eclogites from southwestern Oregon. *Geol. Soc. Am. Bull., 84,* 2471–2488.

Green, D. H. and A. E. Ringwood (1967) An experimental investigation of the gabbro to eclogite transformation and its petrological applications. *Geochim. Cosmochim. Acta, 31,* 767–833.

——— (1972) A comparison of recent experimental data on the gabbro–garnet granulite–eclogite transition. *J. Geol., 80,* 277–288.

Hey, M. H. (1954) A new review of the chlorites. *Mineral. Mag., 30,* 277–292.

Hunt, J. A. and D. M. Kerrick (1977) The stability of sphene, experimental redetermination and geologic implications. *Geochim. Cosmochim. Acta, 41,* 279–288.

Hunziker, J. C. (1969) Rb–Sr-Alterbestimmungen aus den Walliser Alpen Hellglimmer—und Gesamtgesteinsalterswerte. *Eclogae geol. Helv., 62,* 527–542.

——— (1970) Polymetamorphism in the Monte Rosa, Western Alps. *Eclogae geol. Helv., 63,* 151–161.

——— (1974) Rb–Sr and K–Ar age determination and the Alpine tectonic history of the western Alps. *Mem. Ist. Geol. Mineral., Univ. Padova, 31.*

——— and P. Bearth (1969) Rb–Sr Altersbestimmungen aus den Walliser Alpen. Biotitalterswerte und ihre Bedeutung für die Abkühlungsgeschichte der alpinen Metamorphose. *Eclogae geol. Helv., 62,* 205–222.

Ito, K. and G. C. Kennedy (1971) An experimental study of the basalt–garnet granulite–eclogite transition. *Geophys. Monograph Ser., 14,* 303–314.

Kienast, J. R. (1973) Sur l'existence de deux séries differents au sein de l'ensemble "Schistes lustrès–ophiolites" du Val d'Aoste, quelques arguments fondés sur l'étude des roches métamorphiques. *C. R. Acad. Sci. Paris, 276,* 2621–2624.

——— (1976) Etude de paragenèses magmatiques relics et métamorphiques d'un gabbro lié à la série ophiolitique inférieure du Val d'Aoste, Alpes italiennes (abstr.). *Réunion ann. Sci. Terre, Paris,* 241.

Liou, J. G. (1973) Synthesis and stability relations of epidote, $Ca_2Al_2FeSi_3O_{12}(OH)$. *J. Petrol., 14,* 381–413.

———, S. Kuniyoshi and K. Ito (1974) Experimental studies of the phase relations between greenschist and amphibolite in a basaltic system. *Am. J. Sci., 274,* 613–632.

Maresch, W. V. (1977) Experimental studies on glaucophane: an analysis of present knowledge. *Tectonophysics, 43,* 109–125.

Miyashiro, A. (1957) The chemistry, optics, and genesis of the alkali–amphiboles. *J. Fac. Sci. Univ. Tokyo,* Sec. II, *11,* 57–83.

Niggli, E. (1970) Alpine Metamorphose und alpine Gebirgsbildung. *Fortschr. Mineral., 47,* 16–26.

———, W. Frank, F. Purtscheller, F. P. Sassi, B. Zanettin, A. Boriani, M. Frey, A. Montrasio, A. Mottana, R. Potenza, U. Seemann, J. Bocquet, G. V. Dal Piaz, J. C. Hunziker, G. Martinotti and A. Pêcher (1973) Metamorphic map of the Alps: scale 1:1,000,000. *Subcommission for the Cartography of the Metamorphic Belts of the World,* Leiden/UNESCO, Paris.

Nitsch, K. H. (1972) Das P–T–X_{CO_2}-Stabilitätsfeld von Lawsonit. *Contrib. Mineral. Petrol., 34,* 116–134.

——— (1974) Neue Erkenntnisse zur Stabilität von Lawsonit. *Fortschr. Mineral., 51,* 34–35.

Råheim, A. and D. H. Green (1974) Experimental determination of the temperature and pressure dependence of the Fe–Mg partition coefficient for coexisting garnet and clinopyroxene. *Contrib. Mineral. Petrol., 48,* 179–203.

——— and ——— (1975) P,T paths of natural eclogites during metamorphism. A record of subduction. *Lithos, 8,* 317–328.

Ramberg, H. and G. W. deVore (1951) The distribution of Fe^{++} and Mg^{++} in coexisting olivines and pyroxenes. *J. Geol., 59,* 193–210.

Schuiling, R. D. and B. W. Vink (1967) Stability relations of some titanium-minerals (sphene, perovskite, rutile, anatase). *Geochim. Cosmochim. Acta, 31,* 2399–2411.

Taylor, H. P. and R. G. Coleman (1968) O^{18}/O^{16} ratios of coexisting minerals in glaucophane-bearing metamorphic rocks. *Geol. Soc. Am. Bull., 79,* 1727–1756.

Ungaretti, L., A. Dal Negro, F. Mazzi and G. Rossi (1977) Una nuova procedura per l'analisi cristallochimica dei minerali delle rocce. I. Gli anfiboli alcalini (abstr.). *Rend. Soc. Ital. Mineral. Petrol., 33,* 156.

Wetzel, R. (1974) Hornblenden aus der Albit- bis Albitoligoklaszone zwischen Zermatt und Domodossola. *Schweiz. Mineral. Petrogr. Mitt., 54,* 151–208.

Wood, B. J. and S. Banno (1973) Garnet–orthopyroxene and orthopyroxene–clinopyroxene relationships in simple and complex systems. *Contrib. Mineral. Petrol., 42,* 109–124.

Manuscript received, November 23, 1977; accepted for publication, February 18, 1978.